RSC Advances

ROYAL SOCIETY OF CHEMISTRY

www.rsc.org/advances

Growth and synthesis of mono and few-layers transition metal dichalcogenides by vapour techniques: a review

Matteo Bosi

IMEM-CNR, Parco Area delle Scienze 37A, 43124 Parma, Italy
bosi@imem.cnr.it

Abstract

Nanosheet materials such as graphene, boron nitride and transition metal dichalcogenides have gathered a lot of interest in recent years thanks to their outstanding properties and promises for future tecnology, energy generation and post-CMOS device concepts. Amongst these class of materials transition metal dichalcogenides based on molybdenum, tungsten, sulfur and selenium gathered a lot attention because of their semiconducting properties and the possibility to be synthesized by bottom up techniques. Vapour phase processes such as chemical vapour deposition permit to produce high quality layers and to precisely control their thickness. In order to target industrial applications of transition metal dichalcogenides it is important to develop synthesis methods that allow to scale up wafer size, and eventually integrate them with other technologically important materials.
This review will cover all the currently proposed methods for the bottom up synthesis of transition metal dichalcogenides from the vapour phase, with particular emphasis on the precursors available and on the most common semiconductor techniques like metal organic chemical vapour deposition and atomic layer epitaxy. A summary of the most common characterization technique is included and an overview of the growth issues that still limit the application of TMD is given.

Introduction

The continuous improvement of electronic devices, their ubiquitus empoyment in modern society and the opportunties offered by information technology are driven by the continuous scaling down of transistors, mostly based on silicon. Currently, the most advanced computer processors are based on silicon metal-oxide semiconductor field effect transifstors (MOSFET), with gate lengths of 22 nm [1]. Further improvements of device performance will soon approach the limits posed, amongst others, by quantum mechanics effects, by heat dissipation and by shrinking of the gate dielectric. In order to meet the requirements to fulfill Moore's law, scientists are investigating new materials and new concepts that will permit to go beyond the boundaries of current designs. Silicon-germanium (SiGe) and germanium are some of the candidates to push up device performances, since they have higher electron mobility and allows for lower voltages and reduced power consumption, tunneling, and leakage [2]. Strain engineering and high-k gate dielectrics are studied in order to enhance the possilibilities offered by standard materials [3]. Nanostructures and low dimensional materials are also being considered as candidates for novel devices, since they would permit to adopt radical new design concepts [4].
Amongst all the proposed solutions, graphene is the one that attracted most attentions [5]. Its exceptional mechanical, electronic, optical and transport properties have promoted a lot of fundamental and applied research, resulting in a nobel prize assignement and in the development of new physics. Its carriers have mobility of 10^6 $cm^2V^{-1}s^{-1}$ and are Dirac fermions with zero effective mass, making possible to study phenomena related to the quantum mechanics theory in a condensed-matter playground. Integrated circuits based on graphene transistor were demonstrated and high-frequency operation up to gigahertz was demonstrated [6]. Graphene functionalization permitted to realize novel chemical and biological sensors [7] and is also being considered for hydrogen conversion and storage [8].
Despite all these opportunities, graphene has several major drawbacks such as the lack of an electronic bandgap that makes certain kind of applications, for instance logic circuits, very difficult to develop: a graphene transistor cannot have the two conventional on and off states, it cannot be completely switched

off, it has more energy leakage and produces more heat. Bandgap opening is possible throught bandgap engineering (by nanostructuring, chemical functionalization or by applying a high electric field) but this step adds another level of complexity and degrades material properties. Graphene intrinsic defects and the presence of surface adatoms degrades the carrier mobility. Moreover it is chemically inert and functionalization, necessary to make it reactive to selected molecules, results in loss or degradation of several of its properties. These drawbacks fostered the research on alternative materials with similar structure and characteristics.

There is a wide variety of materials that can be thinned down to monolayer like graphene, exhibiting strong in-plane bonds and weak interplane interaction. The list includes transition metal dichalcogenides (TMD), silicene [9], germanene [10] and boron nitride [11]. The properties of these materials depend on their dimension rather than their lateral size and, due to their novelty and excellent electronic properties, they are considered an exiting field for new research.

TMD are materials with chemical formula MX_2, where M is a transition metal of group 4-10 (Nb, Ta, Mo, W, etc.) and X a chalcogen such as S, Se, Te. They are studied since long time and, in bulk form, were grown since 1970 [12], [13], [14], [15]. The typical crystal structure (Fig. 1) consists in a stack of a transition metal layer between two chalcogen layers and it can be described as a Van der Waals solid with strong (covalent) bonds in 2D plane, while the interaction between different planes is much weaker. Their symmetry is hexagonal or rhombohedral, with atoms arranged in octahedral or trigonal prismatic coordination.

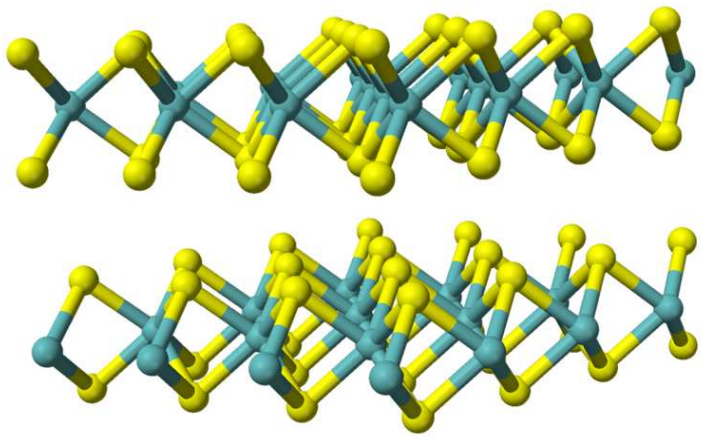

Fig. 1: typical lattice stacking of transition metal dichalcogenide.

TMD bulk material can be exfoliated with different methods such as scotch tape [16], solvents [17] or lithium intercalation [18]. More than 40 combinations of M and X were observed [19], with very different characteristics and a large range of electronic properties from metallic to semiconducting to superconducting. Bulk properties differ significantly from the ones of low dimensional, few layer stacks of TMD: for example the bandgap may change from indirect (bulk) to direct (monolayer), resulting in strong enhancement of optical absorption and emission [20]. When TMD are thinned down to monolayers, they have the same honeycomb structure of graphene and posses very similar properties, but the most important difference is that they exhibit a finite direct bandgap, from 1 to 2 eV, making 2D TMD ideal candidates for electronic devices, logic circuits, detectors, optoelectronic, photovoltaic, energy storage and catalytic applications [21].

Novel properties are observed in monolayer TMD, such as valley polarization: conduction and valence bands of TMD monolayers present two inequivalent valleys at points K and K0, giving a new degree of freedom to carriers. New device concepts can be based on valleytronics, addressing the carriers by their valley index and permitting a control of information using circular polarized light [22]. Moreover, spin–valley coupling may occur, offering a feature that may lead to completely new device design [23].

TMD electronic and semiconducting properties (Table 1) make them ideal candidates for the realization of digital electronic devices, FET and transistor, with the possibility to achieve high on/off current ratio [24].

Important milestones were achieved with TMD, such as the development of a top-gated MoS_2 FET with mobility of 60-70 $cm^2 V^{-1} s^{-1}$ and on/off ratio of 10^8 at room temperature [25], inverters with gain between 2 and 16 [26] [27], phototransistors and photosensors [28], [29], gas and biological sensors [30]. The trend is now to integrate different building blocks into a single device and to fabricate high performance CMOS based circuits [31].

The continuous advance of personal portable devices, smartphones over all, is pushing researchers to develop flexible high performance electronics. Low dimensional materials such as graphene and TMD have high mechanical strength and can be deformed up to 10% before breaking and, thanks to the low dimensionality, they can be deposited or transferred on flexible substrates: this makes TMD ideal candidates for the next generation of portable devices and indeed the first demonstration of flexible devices with these materials already occurred [32], [33].

Nowadays most of the optoelectronic devices are made from III-V and III-N compounds. Their great success is due to the possibily to form ternary compounds such as $In_xGa_{1-x}As$, $In_xGa_{1-x}N$, $Al_xGa_{1-x}As$ etc with different composition. it is thus possible to fabricate lattice matched and mismatched heterostructures, to tune the bandgap, optical emission, absorption, electron properties, etc, and to realize complex devices such as LED, solar cells, photodetectors. TMD and 2D nanosheets such as graphene and boron nitride can be considered as a new class of materials that in principle would permit to obtain ternary compounds and stacked layers similar to the one realized for III-V compounds. Theoretical models predict that mix of TMD is thermodynamically stable [34] and the bandgap of a ternary alloy can be continuously tuned [35] [36]. Stacks of exfoliated 2D material were combined to realize LED by Van der Waals heterostructures [32].

Table 1: electronic proprties of nanosheet materials (adapted from [37]**)**

material	type	monolayer bandgap (eV)	Mobility (cm^2/Vs)
graphene	semi metallic	/	$2x10^5$
silicene	semi metallic	/	$1x10^5$ (theory)
germanene	semi metallic	/	$1x10^5$ (theory)
BN	insulating	5,2	
MoS2	semiconducting	1,8	200 (monolayer)
MoSe2	semiconducting	1,5	50 (exfoliated)
MoTe2	semiconducting	1,1	50 (bulk)
WS2	semiconducting	1,9 - 2,1	100-200 (bulk)
WSe2	semiconducting	1,7	100-500 (bulk)
WTe2	semiconducting	1,1	20 (bulk)
TaS2	metallic super conducting	/	
TaSe2	metallic super conducting	/	
NbS2	metallic super conducting	/	
NbSe2	metallic super conducting	/	

Most of TMD devices developed so far were realized from mechanically exfoliated sheets. Although flakes quality is very high and excellent proof of concepts may be obtained in this way, the method pose critical limits on large scale production. In order to target TMD industrial applications it is mandatory to develop reliable and high-throughput deposition techniques on large area substrates, and compatibility with the current systems and processes could be a tremendous added value. Control of the precursors flow in the vapour phase through the use of gases or controlled evaporation of liquid precursors would permit to increase deposition reproducibility. Chemical Vapour Deposition (CVD) and Atomic Layer Deposition (ALD) are nowadays the most used processes to realize almost all kind of electronic devices with the current used materials (Si, Ge, III-V, III-N, oxides, etc): it would be highly desirable to develop TMD synthesis processess

that share the same deposition equipments used for other materials, since it could open the possibility to directly integrate TMD with other materials.

Not all TMD are technologically interesting, since most of them are not stable in standard conditions and reacts rapidly with atmosphere, losing their peculiar properties. The most promising, and the ones on which this review will focus, are MoS_2, $MoSe_2$, WS_2 and WSe_2, thanks to their peculiar electronic, optical and chemical properties and the possibility to synthesize them by bottom up techniques.

Several papers were already published on the most important properties, applications and synthesis of TMD [19], [37], [38], [39], [40], [41] but a comprehensive review on the different vapour phase deposition techniques, in particular with focus on CVD and ALD has not been proposed, yet.

An analysis of the growth methods, processes and precursors for this novel class of 2D materials is extremely important in order to understand the best routes to obtain the highest quality material and the most feasible way to realize TMD nanosheets. For example, the controlled and reproducible synthesis of monolayer TMD with low defects and crystallinity, the deposition scalability to large area, the fabrication of TMD heterostructures and the possibility to integrate them with other materials are still open issues to be addressed. Providing technological solutions for the growth of TMD would pave way towards the realization of new applications and device based on these materials.

TMD characterization and properties measurements

TMD characterization, applications and device development have been deeply analyzed in dedicated reviews and papers, to which the reader is addressed for details [24], [37], [38], [41], [42], [43], [44]. However, in order to give a complete overview of this class of materials, a brief summary of the most common characterization techniques will be provided in this section.

Raman spectroscopy and photoluminescence are considered the most useful and reliable techniques to identify the numbers of layer in both exfoliated and synthesized TMD. Optical interference and Atomic Force Microscopy (AFM) are also used to exacly determine the layer numbers but, although they can provide precise results, they have limited throughtput and are more time consuming. In order to develop synthesis on large area substrates and to target mass production, fast and reliable characterization techniques are needed, and Raman and PL can succesfully meet these requirements.

Raman spectroscopy is considered a powerful tool to determine the number of layers: the vibrational modes of TMD flakes are strongly influenced by the thickness, since any additional layer beyond the first interacts with the bottom layer and change energy, width and amplitude of the peaks [45]. Only two peaks are usually permitted in Raman backscattering geometry of few-layers TMD, namely E^1_{2g} and A_{1g}, related to the in-plane and out-of-plane vibrations of M and X atoms, respectively. As the layer number increase, the out of plane vibrations A_{1g} are dampened, leading to a blue shift. The E^1_{2g} peak, instead, undergoes a red shift due to the relaxation of in-plane phonon modes. Moreover, A_{1g} modes are sensitive to carrier density and doping, resulting in red shift and peak broadening, respectively [24]. Table 2 summarizes the expected Raman peak position of bulk and monolayer TMD.

	Raman peak	Peak position (cm^{-1})		REF
		1L	bulk	
MoS_2	E^1_{2g}	384	383.5	[45]
	A_{1g}	405	408.6	
$MoSe_2$	E^1_{2g}	287.2	286	[45]
	A_{1g}	243	240.5 – 242.5	
WS_2	E^1_{2g}	356	355.8	[46]
	A_{1g}	418	420	
WSe_2	E^1_{2g}	250	248	[45], [47]
	A_{1g}	250	250.2	

Table 2: Raman peak of most common TMD in monolayer and bulk form.

One of the most important characteristics of monolayer TMD is the strong enhancement of PL signal with respect to bulk emission [20]. As discussed in the previous section, bulk TMD are indirect bandgap materials: the indirect bandgap is due to a transition from the top of the Γ point valence band to the bottom of the conduction band, between Γ and K point. As the number of layers decrease down to one, the indirect bandgap energy increases and cross the direct gap, that remains in the same position. This is the reason for the strong enhancement of the emission signal, up to 10-20x, coupled to a peak blue shift.

thanks to micro-PL mapping, different zones of a single flake can be analyzed in order to identify defects or the presence of additional layers.

	PL Peak position (eV)		REF
	1L	bulk	
MoS_2	1.8	1.2	[45]
$MoSe_2$	1.82	1.1	[45]
WS_2	1.95	1.3	[48]
WSe_2	1.65	1.2	[45]

Table 3: main PL peaks of most common TMD in monolayer and bulk form.

Methods for TMD nanosheets synthesis

Top down

Top-down methods for TMD nanosheets synthsis can produce high quality monolayer samples at low cost and are very convenient for fundamental research and for the realization of proof-of-concept devices.
There are basically two top down strategies adopted: mechanical exfoliation through Scotch tape and liquid methods, which can be subsequently divided in two categories: lithium intercalation and solvent-assisted sonication.
Since most TMD, and in particular MoS_2, $MoSe_2$,WS_2 and WSe_2, are available in bulk form, single layers can be exfoliated using the Scotch tape methods, similarly to what is done on graphene. Exfoliated flakes up to 10 μm wide and high crystallinity can be obtained and are usually identified using optical microscopy, considering the color contrast given by layers with different thicknesses on SiO_2 (Fig. 2) [49]. However, despite these results, the scale up of Scotch tape method is extremely difficult and the throughtput is very limited.

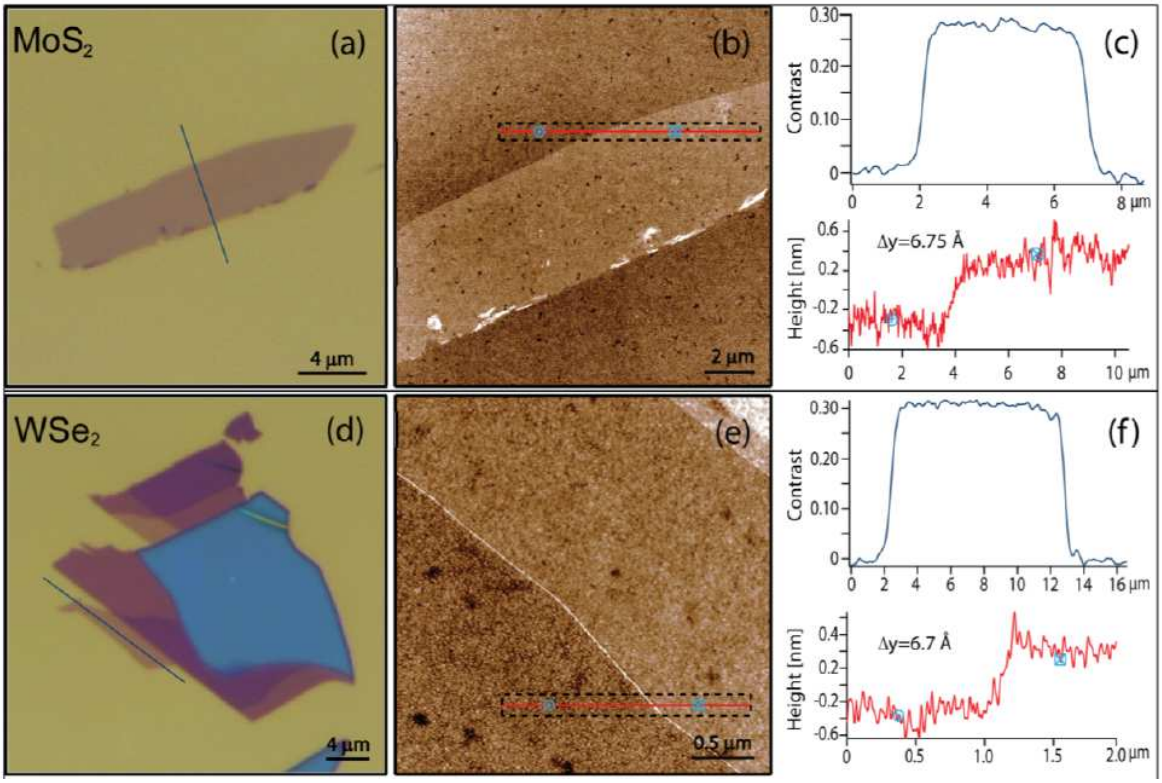

Fig. 2 Optical and atomic force microscopy images of dichalcogenide nanolayers deposited on 270 nm SiO_2 with corresponding contrast and height profiles of monolayers: (a)–(c) for MoS_2, (d)–(f) for WSe_2 and (g)–(i) for $NbSe_2$. Contrast and height profiles of monolayer flakes are taken across the black lines drawn on optical images, and red lines on AFM images. Measured thicknesses correspond well with interlayer distances in dichalcogenide crystals. Observed optical contrast is in the 25–30% range for MoS_2 and WSe_2 and is slightly lower that the values predicted in the model. In the case of NbSe2 optical contrast is in the 5–10% range. [49]

TMD can be exfoliated by ultrasonic treatment in appropriate solvents or by using surfactants (Fig. 3) [17]: sonication usually results in crystal flakes with dimension of a few hundreds nanometers [50], [51]. A more viable solution is to utilize lithium containing compounds that intercalate into atomical layers, followed by a

reaction in water, that separates the sheets by producing H_2 [18], [52]. Althought exfoliation in liquid permits to obtain high yield of monolayes dispersed in a solution that can be adopted for applications such as electrochemical energy storage, catalysis, sensing, in ink-jet printing or to obtain composites and hybrids by mixing different solutions with different materials, its main disadvatages are the small size of the obtained flakes, that can limit some applications where large area flakes or films are needed. The challenges to be addressed are the yield enhancement of single layers (most of the flakes are few-layers) and the control of the lateral dimensions of the exfoliated sheets.

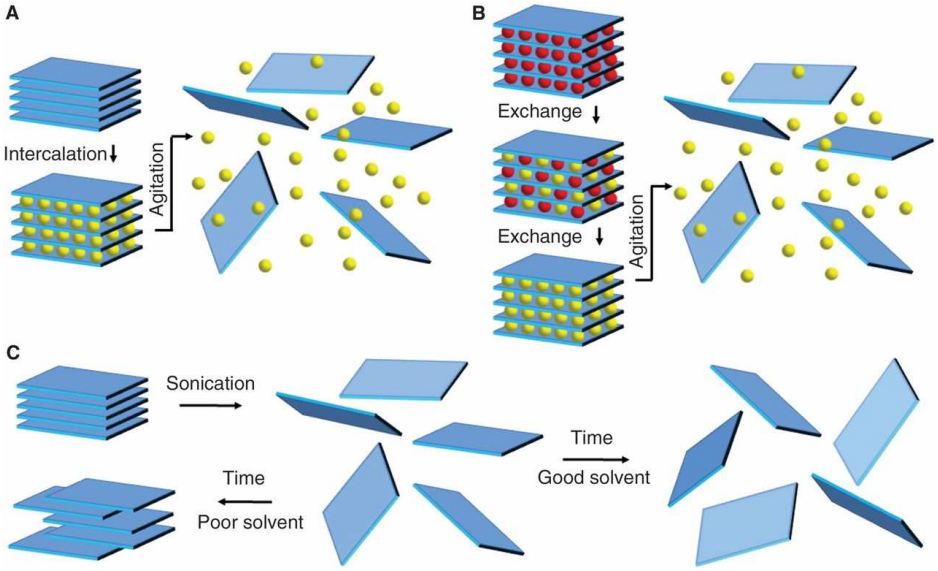

Fig. 3 Schematic description of the main liquid exfoliation mechanisms. (A) Ion intercalation. (B) Ion exchange. (C) Sonication-assisted exfoliation. From V. Nicolosi, M. Chhowalla, M. G. Kanatzidis, M. S. Strano, and J. N. Coleman, "Liquid Exfoliation of Layered Materials," Science (80-.)., vol. 340, no. 6139, pp. 1226419–1226419, Jun. 2013. Reprinted with permission from AAAS.

Since this review will mainly focus on gas phase methods, the reader is addressed to other reviews for details about the above cited top down methods. For example MoS_2, $MoSe_2$, WS_2, $NbSe_2$, WSe_2, VSe2 and $MoTe_2$ obtained by mechanical exfoliation are reported in [53] [54], [55], [56], [57]; a comprehensive list of solvents used for the liquid exfoliation is cited in [50] while lithium intercalation is discussed in [58], [59].

Bottom up

In order to integrate TMD in existing electronics and to design new kind of devices it is mandatory to obtain a good control in terms of number of layers (one layer as opposed to few-layers), crystal quality (absence of defects, grain boundaries), lateral dimension of sheets and scalabilty to large area substrates. Top down methods, even if permit to produce very high quality material, fail to fulfill most of these requirements. For this reason several techniques were developed with a bottom up approach, starting from TMD costituent elements to controllably synthesize nanosheets over a given substrate.

Most of the proposed processes utilize one or two of the TMD consituent elements (metal and sulfur/selenium) in vapour form, transporting the selected species over the substrate with a carrier gas. This permit, in principle, to achieve a good control over the gas composition and, through flowdynamic optimizations obtained with chamber / tube design, to deliver the precursors in a homogeneous way over all the substrate area: large area scalability, uniformity and thickness control are routinely achieved for thin films deposited by CVD and can potentially be obtained also for monolayer TMD.

CVD is a widely used technique in material science and it is commonly employed to deposit a large class of semiconductors, metals, oxides, etc on a variety of substrates. Only recently it was applied for the synthesis of low dimensional materials, such as graphene and TMD. Li et al [60] were the first to demostrate large scale deposition of graphene utilizing methane on copper foil and later a variety of papers followed on TMD and boron nitride nanosheets.

Depending on the particular setup, the gas flow can be carefully controlled through the chamber design and a good flowdynamic optimization can, in principle, guarantee an efficient transport of species, good homogeneity, easily scale up to large area and excellent reproducibility. For these reasons CVD is one of the most promising techniques to synthesize monolayers TMD on large area with controlled thickness, good crystallographic quality and excellent electronic properties.

ALD is a modified CVD technique in which the two precursors are delivered separately in the growth chamber. It was invented by T. Suntola in 1974 [61] and was originally used to deposit ZnS film for electroluminescent devices. ALD is nowadays very common for oxides growth and for conformal deposition on nanostructures, patterned substrates, high aspect ratio structures such as trenches or pillars, etc, and it is largely used for the deposition of high-k oxides.

A single ALD growth cycle consists in: injection of precursor 1, purge with inert gas, injection of precursor 2, purge with inert gas. Excess reactants and reaction by-products are evacuated during purge cycles and the surface reactions during precursors supply are self-limited: if the substrate surface is sufficiently reactive to the precursor and if the precursor does not bond with itself, one ALD growth cycle should in principle deposit a single monolayer of the selected specie: uniform films with excellent conformality can be thus deposited even onto complex-shaped large area substrates. For this reason, ALD should be considered as one of the most promising technique for the deposition of TMD, because theoretically it would permit to tailor the number of deposited layers by defining the number of cycles. Despite its potential, ALD is still not so widespread for TMD, mainly because of a lack of suitable chemistry [62]. Nevertheless, several groups used ALD also for the deposition of metals or metal oxides of controlled thickness to be further sulfurized or selenized by other techniques.

Before discussing the details of the different synthesis procedures, it is to be noted that most of these techniques share common precursors: it is thus very important to understand which kind of chemicals are available for TMD CVD and their physical properties. Beside the most commonly used S or Se powders or H_2S gas for chalcogens, there are also less common chemicals worth to be mentioned. Also, M or MO_x may be deposited on a substrate for further selenization / sulfurization: knowledge on how to control their depoisition is often mandatory to obtain monalyer TMD.

The following section will exaustively discuss the precursors used for TMD synthesis by CVD. To the best of author's knowledge this summary was never proposed before. The main focus will be on S, Se, Mo and W because MoS_2, $MoSe_2$, WS_2 and WSe_2 are considered to be the most technologically relevant compounds for the realization of devices.

Precursors

Sulfur

Sulfur powders

Sulfur powders are the most used precursor to deliver S to the substrate. S powders are avilable with high purity (up to 99,998%), can be easily handled and are non-toxic: for this reason they are preferred to H_2S. The Material Safety Data Sheet (MSDS) of S reports skin irritation as the only hazard, requires to avoid contact with skin and eyes, formation of dust and aerosols and indicates to provide appropriate exhaust ventilation in places where dust is formed.

S powder melts at 115 °C and evaporates to gaseous sulfur, with vapour pressure reported in Fig. 4: knowing the value of this parameter permits, in principle, to get a better control of the gas phase and to deliver a controlled quantity of precursor towards the substrate. However, the quantity of vapourized sulphur depends also on the mass of powder put in the crucible: for this reason the use of powders as main reagents, even if it is very common due to its simplicity, may pose some problems for reproducibility and control of the deposited layers.

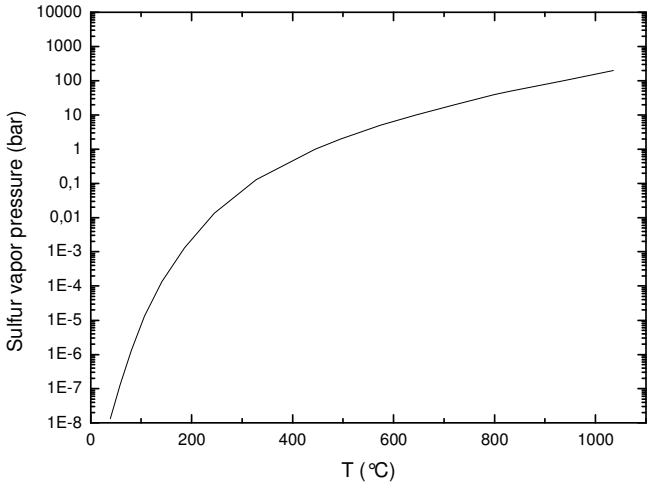

Fig. 4 Sulfur vapour pressure vs temperature (adapted from [63]**)**

H_2S

Hydrogen sulfide is a a colorless gas with characteristic odor of rotten eggs; it is heavier than air, very poisonous, corrosive, flammable, and explosive. It is used as a source for S in the deposition of TMD but its handling requires particular attentions and safety measures (Table 4). MSDS of this substance describes the consequences of exposure to eye, skin and inhalation and should be carefully readed. Flammable range of H_2S is between 4.3% and 46% in air and poses an immediate fire hazard when mixed with air. Distant ignition and flashback are possible and flames or high temperature exposure of the cylinder can cause an explosion. Although its odor is very pungent, it quickly deadens the sense of smell, so the victims may be unaware of its presence until it is too late.

For all these reasons, special care should be taken to design a reactor with H_2S line [64] and it is not so commonly used for the synthesis of TMD but, despite safety drawbacks, several research groups utilize it because the delivery of a gas to the growth chamber is much more controllable than evaporation of solid sources, ensuring higher reproducilibity of the process.

Thanks to its fast decomposition at high temperature, H_2S should be more efficient that elemental S in the growth of TMD, and should help in improving uniformity [65]. Partial pressure of H_2S in the gas phase during TMD growth is usually in the range 10^{-1} – 10^{-2} [66], [67]. H_2S may also act as reducing agent for metal oxides.

Table 4: Sulfur exposure limits

	Limit (ppm)
Short-term exposure limit (STEL)	15
Immediately Dangerous to Life and Health (IDLH)	100

Other sulfur precursors

A few less common S precursors are reported in literature. For example dimethyl disulfide (CH_3SSCH_3, DMDS) was used with $Mo(CO)_6$ to grow by ALD MoS_2 on SiO_2 [62] and 1,2- ethanedithiol ($HS(CH_2)_2SH$), 2-methylpropanethiol ($HSC(CH_3)_3$) were used for the CVD of WS_2 thin films on glass [68]. The sources were heated to 63 °C and 55 °C, respectively. In the cited paper thick nanocrystallince film were deposited: no reports about mono or few-layer of WS_2 were found in literature using these precursors.

Selenium

Selenium powders

Selenium powders are the most common precursor used for the selenization of metals or metal. They are easily handled and are available in pellets (<5 mm particle size) or powders with purity up to 99,999%. On the contrary to S, Se powders must be properly handled because Se is toxic by inhalation and if swallowed. It has severe danger of cumulative effects if the operator is exposed for long time and it must be correctly disposed because it may cause long-term adverse effects in the aquatic environment. Danger of acute Se exposure are described in the MSDS and safety handling precautions must be adopted.
Brooks [69] studied the vapour pressure of solid selenium with quartz Boudon gages, reported in Fig. 5

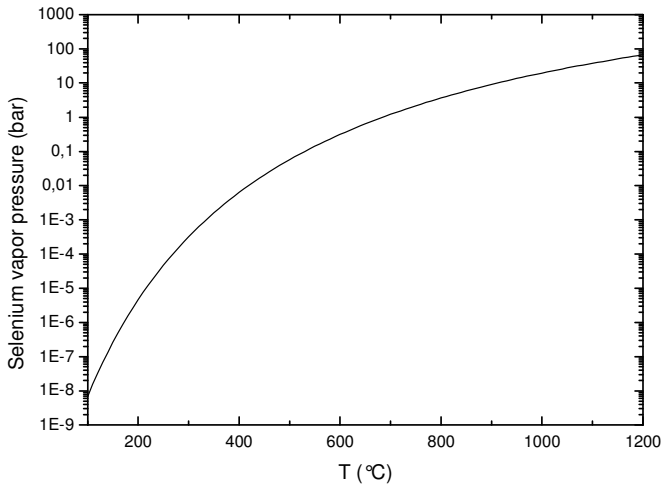

Fig. 5: selenium vapour pressure (adapted from [69])

H_2Se

Hydrogen selenide is a colorless, flammable gas under standard conditions, heavier than air. It is reported to be the most toxic selenium compound and it must be treated and handled with extreme attention, because it may explode in contact with water, it is a flammable gas and may cause flash fire. Due to its high toxicity (Table 5) particular care should be taken to handle the exhaust gases from the growth chamber. Even at extremely low concentrations H_2Se has a very irritating smell, resembling decayed horseradish, and smells of rotten eggs at higher concentrations. Concentrations of 0.3 ppm are readily detected by the nose, but there is no noticeable irritant effect at that level. Concentrations of 1.5 ppm or higher are strongly irritating to the eyes and nose.
However, like H_2S, the odor in concentrations below 1 ppm rapidly disappears because of olfactory fatigue.
MSDS of this compound reports that it is deadly poison by inhalation and a very poisonous irritant to skin, eyes, and mucous membranes. It may also cause central nervous system effects. It has been found that repeated exposures to concentrations of 0.3 ppm are fatal to experimental animals by causing a pneumonitis and injury to liver and spleen.

Table 5 H_2Se exposure limits

	Limit (ppm)
8-hour period	0.05
Immediately Dangerous to Life and Health (IDLH)	100

Due to its high toxicity and the ready availability of safer alternatives, H_2Se is usually not used for the synthesis of TMD, even if it can react with W to form WSe_2 according to the reaction [70] (1) :

$W + H_2Se \rightarrow WSe + H_2$ (at 300 – 400 °C) (1)
$W + (2-x)\ H_2Se \rightarrow WSe_{2-x} + (2-x)\ H_2$

Bozheyev et al [71] have used H_2Se as a selenization agent to prepare WSe_2 thin films 600 nm thick, starting from selenium-rich WSe_{2-x} deposited by reactive magnetron sputtering but, at the best of author knowledge, no other paper was found employing H_2Se for nanosheet TMD synthesis.

Other Se precursors
Beside Se powders several groups are investigating the use of alternative Se precursors. As discussed above, it not straightforward to control Se supply by the use of powders and reproducibilty could be an issue. Liquid Se precursors kept at a definite temperature permit to get a precise control of the vapour pressure and to deliver a well-defined amount of reagent towards the growth chamber by the use of a carrier gas.
The synthesis of WSe_2 was carried out via Metal Organic Chemical Vapour Deposition (MOCVD) using tungsten hexacarbonyl $W(CO)_6$ and dimethyl selenide $(CH_3)_2Se$ as the W and Se sources [72]. Dimethyl selenium is a stable colourless liquid with an unpleasant odour, which hydrolyzes in water and reacts violently with acids and strong oxidizing agents. Its boiling point is 56-58 °C so it can be conveniently used in a MOCVD system. Its vapour pressure was determined by Karlson et al [73] and reported in Fig. 6 .
Film quality and carbon contamination depends strongly on $(CH_3)_2Se$ purity: 99.99% pure $(CH_3)_2Se$ performs better than 99% pure precursor [72].

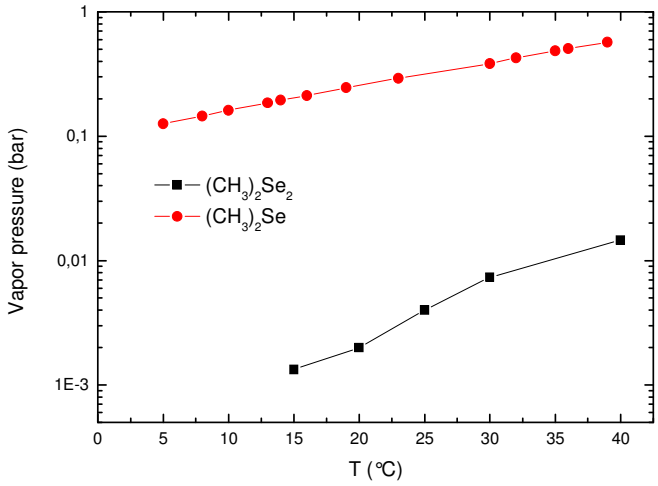

Fig. 6: Vapour pressure of DMSe and DMDSe (adapted from [73]**)**

Diethyl selenide is another metal organic compound that was used to grow WSe_2 thin films [74] but not yet used for the synthesis of nanosheet TMD. It was heated to 60 °C and delivered to the growth chamber by N_2. Its vapour pressure was studied by Tanaka et al [75]. It should as noted that chemical reaction of WSe_2 and Diethyl Selenide could produce H_2Se, so waste gas should be properly handled.
Di-tertbutylselenide and diethylselenide were used by Boscher et al to deposit $MoSe_2$ films using $MoCl_5$ as the other precursor [74] and VSe_2 using using VCl_4 and $VOCl_3$ [76]. In these works the focus was on thin film and not on monolayers: no other paper was found, on the best of author knowledge, about the use of these precursors for 2D TMD.

Mo

Depending on the growth method, Mo can be delivered to the growth chamber starting from metal oxide powders, from vapourized liquids or can be directly deposited in form on thin metallic or metal-oxide layer on the substrate. The use of powders poses the same problems already discussed for S and Se: reproducibility and large scale homogeneity could be an issue. The direct deposition of Mo onto the substrate is in principle the most controllable method, but a precise control of Mo thickness must be achieved. It is often reported that the synthesis of mono or few-layers MoS_2 or $MoSe_2$ depends on the thickness and homogeneity of the initial Mo deposition. Several techniques are available and will be discussed in the following paragraphs to assess this problem, and the same applies to W, too. Thermal decomposition of thyosalts is another route to coat the substrate with a controlled layer of Mo.
Evaporation of liquids, solids or metal-organic Mo compounds such as $MoCl_5$, MoF_6, $Mo(CO)_6$ could be one of the most straightforward methods to integrate Mo into a standard CVD system and to obtain good reproducibility and homogeneity over a large area.

MoO_x powders

In its pure form, molybdenum is a silver-grey metal with melting point of 2623 °C. It starts to weakly oxidate at 300 °C and bulk oxidation starts at temperatures above 600 °C, resulting in molybdenum trioxide.
MoO_3 is produced either by heating MoS_2 or by acidification of aqueous solutions of sodium molybdate with perchloric acid accodring to the reactions (2) [77]:

$$2\ MoS_2 + 9\ O_2 \rightarrow 2\ MoO_3 + 4\ SO_2 \quad (2)$$
$$Na_2MoO_4 + H_2O + 2\ HClO_4 \rightarrow MoO_3(H_2O)_2 + 2\ NaClO_4$$

MoO_3 powders are available with purity up to 99,98%. The vapour pressure of MoO_3 is reported in Fig. 7.

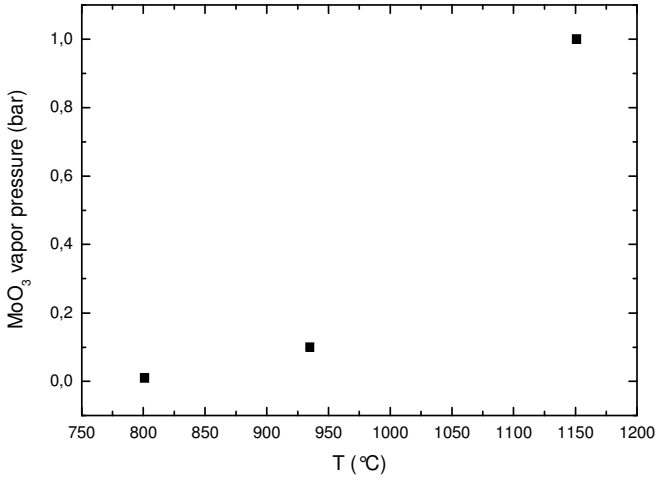

Fig. 7 vapour pressure of MoO_3, adapted from [78]

Mo and MoO_x deposited onto a substrate

In order to achieve a better control over the number of deposited layer and to scale up to large area substrates one possible route is to start from a controlled Mo or MoO_x layer deposited onto a substrate and then convert the metal to MoS_2 or $MoSe_2$ throught a controlled sulfurization or selenization. Since the final number of layer of the TMD is controlled by the number of layers initially deposited on the substrate , it is extremely important to get a precise control over the metal thickness and a good homogeneity over the substrate.

Several techniques are used to deposit a thin Mo film onto a variety of substrates (Si, SiO_2, sapphire, Cr, Au, etc), the most common being e-beam evaporation and sputtering.The thickness of the deposited layer is usually monitered through a quartz microbalance.

An alternative starting layer is MoO_3 deposited by evaporation [79], because this oxide has a lower evaporation temperature with respect to Mo and it is more easily sulfurized / selenized. In order to increase reliablity and control over the number of Mo layers, several groups used ALD with different kind of precursors: this is in principle the best technique control the thickness. There are different precursors available for CVD deposition of either Mo or MoO_3 layers, which will be discussed in the following paragraphs.

$Mo(CO)_6$

Molybdenum hexacarbonyl ($Mo(CO)_6$) can be used with water and ozone to deposit thin MoO_3 films throught ALD. This precursor is solid at room temperature and very volatile, with a melting point of 150 °C and boiling point of 156 °C. It has a vapour pressure of about 0.10 – 0.15 mbar at room temperature, so it is a convenient precursor for CVD.

Diskus et al. [80] used $Mo(CO)_6$ to deposit MoO_3 layers on single crystalline Si(111) and soda lime glass. $Mo(CO)_6$ was kept at room temperature and delivered to the growth chamber with the use of N_2. An onset decomposition of 163 °C was determined for $Mo(CO)_6$. After 1000 cycles the film thickness was between 35 and 75 nm: fine control over layer thickness can thus in principle be obtained.

$MoCl_5$

Molybdenum (V) chloride ($MoCl_5$) is a volatile solid that melts at 194 °C and boils at 268 °C, available with purity up to 99,99%. Its vapour pressure is 1.75 torr at 25°C and 131 torr at 250°C. The compound is very air-sensitive and care should be taken to load the powder into the growth chamber [81]. It is toxic by ingestion, an irritant to skin, and may react with water to produce corrosive hydrochloric acid and toxic fumes.
1-50 mg of $MoCl_5$ are generally used as powders for the growth of MoS_2 along with S powders [82], [83] but $MoCl_5$ is also used for the ALD of MoS_2 with H_2S as the other precursor [84]. For the ALD process, in order to have a suitable vapour pressure, $MoCl_5$ source was kept at 120 °C.

Other Mo precursors

Molybdenum(VI) fluoride (MoF_6) is colourless solid, with a melting poing of 17,5 °C and a boiling point of 34 °C. It is highly unstable toward hydrolysis and reacts violently with water, with the release of toxic HF and molybdenum oxides.
It was used as precursor for ALD of atomic Mo layers with Si_2H_6 as the other reactant [85]. It was also used to deposit thin films of MoS_2 by CVD using H_2S as the other precursor [86], [87] but no reports about the direct synthesis of low dimension TMD were found in literature.
Bis(tert-butylimido)-bis(diethylamido)molybdenum[$(tBuN)_2Mo(NEt_2)_2$] and bis(tert-butylimido)-bis(di-isopropylamido)molybdenum [$(tBuN)_2Mo(NiPr_2)_2$ were used for ALD of molybdenum nitrides [88] but no evidence of a suitable chemistry was found for suflide / selenide compounds.

Thiosalts
Ammonium tetrathiomolybdate $(NH_4)_2MoS_4$ is a compound that contains both Mo and S, prepared from molybdate solutions $[MoO_4]^{2-}$ with hydrogen sulfide in the presence of ammonia [89]. It is solid at room temperature, available with purity up to 99.99%. It is usually added to polar organic solvents such as dimethylformamide (DMF): the solution is spinned onto the substrate andused as starting point to form MoS_2 by sulfurization [90]. The drawback of this precursor is the difficulties to obtain a uniform $(NH_4)_2MoS_4$ film: the thickness of the deposited layer controls the number of MoS_2 layers that will be produced by the subsequent annealing and the scale up to large area is very difficult. Moreover, the presence of C residues from the solvents may reduce the incorporation of S, thus leading to defective or polycrystalline layers.

W
W is usually deposited in form of a thin layer on a substrate, used in form of oxide powders or delivered trough vaporization of solids or liquid to the gas chamber. All the argumentations discussed above for Mo remain valid for W.

W and WO_x deposited onto a substrate
A thin WO_3 layer can be deposited onto a substrate (SiO_2,sapphire, graphene/SiC) by thermal evaporation or sputtering [91], [92]. ALD of W or WO_3 layers is reported with WF_6 [93], [94], [95] or $W(CO)_6$ [96]. Although few works were found about the sulfurization / selenization of W or WO_3 layers deposited by ALD , the layer control, homogeneity and scalability offered by this technique could significantly help to further develop WS_2 and WSe_2 synthesis.

WO_3 powders
WO_3 is available in powders with purity up to 99,995%. Its melting point is 1,473 °C and its vapour pressure is reported inFig. 8. WO_3 are obtained from W ores by reactions with alkalis.

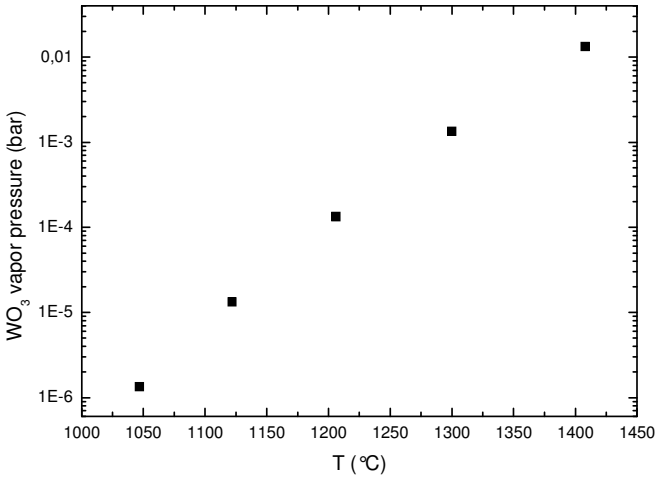

Fig. 8 WO_3 vapour pressure, adapted from [97]

Other W precursors

$WOCl_4$, $WOCl_6$, WCl_6

Tungsten hexacarbonyl ($W(CO)_6$), tungsten (VI) chloride (WCl_6) and Tungsten oxychloride ($WOCl_4$) were used as precursors for WS_2 CVD synthesis along with S sources $(CH_3)_2Se$, 1,2- ethanedithiol $[HS(CH_2)_2SH]$ and 2-methylpropanethiol $[HSC(CH_3)_3]$. The W precursors were kept in stainless steel bubblers at temperatures of 165, 245 and 176 °C, respectively [68], [72].

WCl_6 , kept at 100 °C in a stainless steel bubbler, was used for CVD of WS_2 with H_2S [98].

Novel sources such as $WH_2(iPrCp)_2$ and WH_2 $(EtCp)_2$ were used for CVD synthesis of W containing films, including WO_3 and WC_x and WNC_x. They have the advantage to be oxygen free and to have a low onset temperature of 350–400 °C [99], [67]. However, no reports about the use of these precursors for the direct synthesis of WS_2 or WSe_2 were found.

Precursors for other elements

MoS_2, $MoSe_2$, WS_2 and WSe_2 are the most widely synthesized compounds but there are also a few literature reports dealing with other TMD bottom up synthesis. For example Boscher et al. [76] tried to synthesise VSe_2 by atmopsheric pressure CVD using vanadium tetrachloride (VCl_4), vanadium oxytrichloride ($VOCl_3$) and butyl selenide but no significant results were obtained.

$MoTe_2$ and ReS_2 were synthesized using respectively Te pellets with Mo powders [100] and Re and S powders [101].

Methods

Table 6

Chalcogen \ Metal		Metal deposited on substrate			Metal in vapour phase	
		M	MO_x	thiosalt	MO_x	other
Powder	S	X	X	X	X	X
	Se	X	X		X	
Gas	H_2S		X			X
other						X

Table 6 summarizes the combinations of different metals and chalcogen precursors used in literature for the bottom up synthesis of TMD.
The methods currently used can be summarized in two big categories:

- synthesis of TMD from gaseous precursors in the vapour phase, supplied from powder, liquids or directly from H_2S.
- sulfurization or selenization of the metal deposited, in different forms, onto a substrate (thin metal or metal-oxide layer, thiosalt layer).

The most commonly adopted setups used for these methods are sketched in Fig. 9. In some cases standard CVD / ALD equipment is also used, in particular when liquid or gaseous precursor are adopted. In this case the use of mass flow controllers permits to control the gas phase composition more precisely. In the following paragraph the various methods will be discussed and analyzed.

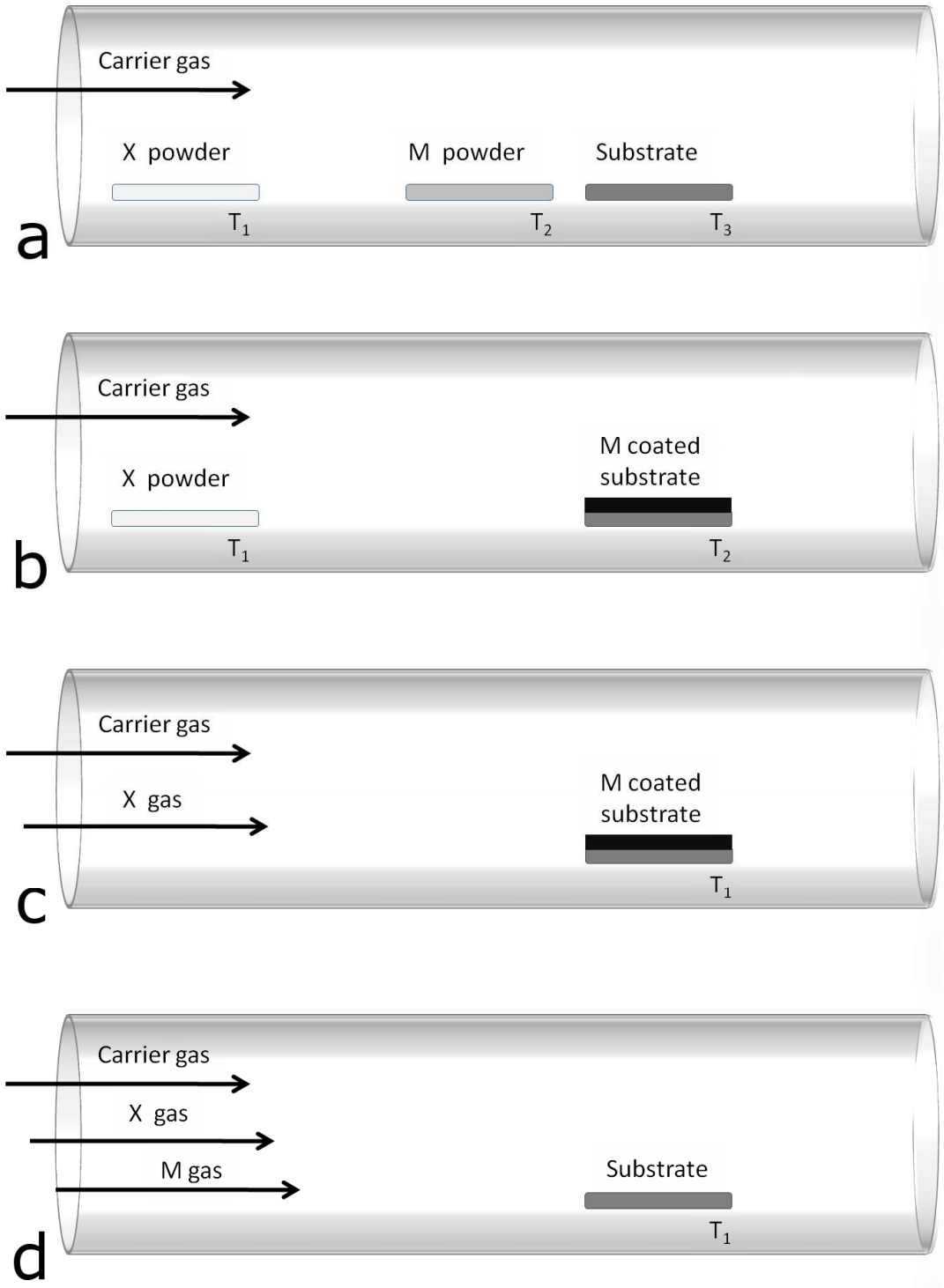

Fig. 9 Schematics of the most common methods used to deposit TMD from vapour phase. Metal (M) and Chalcogen (X) powders. b) metal or metal oxides deposited on substrate and chalcogen powders. c) metal or metal oxides deposited on substrate and chalcogen supplied as gaseous precursors. d) Metal and chalcogen compounds supplied by gaseous precursors

Synthesis of TMD with both precursors supplied from the vapour phase

Metal and chalcogen powders

Due to the simplicity of the setup, of the availability and ease of handling of the precursors, a lot of research groups still synthesize TMD using vapour phase reactions between MO_x and chalcogen powders: even if high quality flakes were obtained and several proof-of-concept devices were realized starting from materials deposited with these techniques, control of layers number, scalability to large area and reproducibility are still an issue.

For the growth of MoS_2 or WS_2 usually 0.5 - 1 grams of S powders are placed in a crucible 7-15 cm away from the substrate, heated independently at temperatures ranging from 100 to 200 °C and delivered, in form of vapours, to the substrate. Sulfur vapour pressure at this temperature corresponds to about 10^{-2} -1 torr. Because sulfur evaporates very fast at high temperature, some authors report the use of two different crucibles, placed at different temperatures and distances from the substrate [102]: the nearest crucible starts to supply S by sublimation at lower temperatures, while the second one supplies S via evaporation before the entire consumption of the first source at higher temperatures occurs. This design assures the continuous supply of reagent during the whole process.

Se powders (0,5 – 1 g) are also usually placed upstream in the growth tube (10-20 cm away from the substrate) and Se vapours are transported to the substrate by a carrier gas. The powders are typically heated at 250-300 °C, corresponding to a vapour pressure in the range 10^{-2} - 10^{-1} torr, according to Fig. 4.

Since the synthesis of TMD occurs between 650 and 800 °C, careful furnace temperature profile control / measurement or additional heaters outside the main growth chamber are usually adopted to control the vaporization of S or Se powders at lower temperatures. Synthesis at both atmospheric pressure and low pressure (1 – 500 torr) is reported [40].

MoO_3 and WO_3 powders (about 0.5 – 1 g) for metal precursor supply are usually placed in a crucible in the high temperature zone of the growth furnace. Mo is usually placed near the substrate or directly underneath it while W, having a lower vapour pressure, it is heated farther from the substrate to temperatures up to 1070 °C , some hundreds degrees higher than the temperature used to synthesize WS_2 [103], [104].

MoO_3 and WO_3 powders are initially reduced to volatile suboxides MoO_{3-x} or WO_{3-x} by S vapours and are then transported to the substrate, where they further react with S vapour to form MoS_2 or WS_2 [104], [105].

The proposed reaction mechanism for Mo is:

$$2MoO_3 + S \rightarrow 2\ MoO_{3-x} + SO_2 \quad (3)$$

$$2\ MoO_{3-x} + (7–x)\ S \rightarrow 2\ MoS_2 + (3-x)\ SO_2$$

with the formation of MoO_2 as an intermediate phase when x = 1.

MoS_2 and WS_2 are usually grown in inert N_2 or Ar athmosphere, because S is a strong reducing agent and it is sufficient to reduce MoO_3 or WO_3 to suboxides. However, Se chemical reactivity is much lower than S one and a suitable reducer agent is required for the suboxide formation. For this reason the synthesis of $MoSe_2$ and WSe_2 from oxide powders necessarily requires the addition of H_2 to the gas phase: without H_2 the growth of $MoSe_2$ or WSe_2 does not occur [27]. Even the addition of some percent of H_2 to the gas phase is reported to be sufficient to produce MoO_{3-x} or WO_{3-x} and it may also have a role in the nucleation of flakes on the substrate [106].

Thermodynamic calculations have confirmed the importance of H_2 for the selenization of Mo and W, according to the reaction [107]:

$$WO_3 + 3Se + H_2 \rightarrow WSe_2 + H_2O + SeO_2 \quad (4)$$

The reaction between metal and chalcogen powders may lead to the formation of nanoparticles or nanorods, as opposed to monolayer nucleation. In order to reduce the presence of unwanted structures and to promote large area growth of high quality and continuous monolayer TMD, pretreatment of the substrate surface with aromatic molecules such as reduced graphene oxide, perylene-3,4,9,10-tetracarboxylic acid tetrapotas- sium salt (PTAS), perylene-3,4,9,10-tetracarboxylic dianhydride (PTCDA) was proposed. These substances were diluted in water and a droplet was spun on the substrate surface, followed by drying at 50 °C [105].
A more comprehensive study about the role of seeding promoters for 2D growth of MoS_2 was proposed by Ling et al. [108], by using different aromatic and inorganic molecules on the substrate. They verified that the use of PTAS as seeding promoter permits to obtain large area, continuous and high quality MoS_2 monolayers already at 650 °C, while only nanoparticles were achieved in the same conditions without PTAS. An optimum seed concentration of different aromatic organic molecules (Table 7) can also promote the growth of monolayer MoS_2, while the investigated inorganic particles were not effective. Several promoters may be thermally evaporated on the substrate, permitting to achieve a better control over TMD nucleation, even permitting to pattern the substrate, with respect to the use of aqueous solutions.

	Seeding promoter	Temperature	Thickness / quality
Organic	PTAS	> 600	Monolayer / excellent
	F_{16}CuPc	> 430	Monolayer / excellent
	PTCDA	> 450	Monolayer / good
	CuPc	> 430	Monolayer / good
	DBP	350-450	Monolayer / good
	CV	205	Monolayer / good
	NAA	200	Monolayer / good
	Spiro-TPD	> 280	Monolayer / fair
	TCTA	> 410	Monolayer + multilyer / fair
	BCP	240 / 300	Monolayer + multilyer / fair
	TPBI	>350	Monolayer + multilyer / poor
	Spiro-2-NPB	>390	Monolayer + multilyer / poor
	$Ir(ppy)_3$	>300	Monolayer + multilyer / poor
Inorganic	Al_2O_3		Nothing / bad
	HfO_2		Nothing / bad
	5 Å Au		Particles / bad
	Silicon		Nothing / bad

Table 7 Seeding Promoters used in MoS 2 Growth (adapted from [108], reader is addressed to the reference for explanation of promoters abbreviations).

In order to control the nucleation of 2D TMD without the use of seeding layers or precursor, an appropriate cleaning and storage of the substrate may be required. Zande et al. [109] grew monolayer MoS_2 on SiO_2/Si by cleaning the substrate in acetone, isopropanol H_2SO_4/H_2O_2 (3:1) and 5 min of O_2 plasma in ultrahigh pure N_2. Higher monolayer yield was obtained by using fresh precursors and ultraclean substrates, with minimized air contamination during storage: the use of uncleaned substrates and / or old precursors reduced significantly yield and reproducibility.

Another proposed powder for the growth of MoS_2 is $MoCl_5$ [110], placed in the hot zone of the furnace and several cm away from the substrate, with 1 g of sulfur powder used as sulfurizing agent. The number of MoS_2 layers was found dependent on the weight of $MoCl_5$ placed in the crucible.
Bulk $MoTe_2$ was synthesized using Mo powder and Te pellets [100] at a temperature of 1150 °C. A long growth (1.5 weeks) and a controlled cooling permitted to obtain crystals that were later exfoliated by scotch tape and transferred to SiO_2/Si wafers. Single crystals of ReS_2 were grown with Br_2 as a transport agent [101] at 1060-1100 °C. The bulk crystal was exfoliated to bilayers for further analysis.
By this method vertical and in-plane heterostructures from WS_2/MoS_2 monolayers were obtained [111]: MoO_3 powders were placed in front of the wafer, while a mix of W and Te were deposited on it for the growth of WS_2. The addition of Te promotes W melting during the growth. S powders were put in a zone at lower temperature. MoS_2 and WS_2 were grown sequentially thanks to the difference in their nucleation and growth rates, and the formation of $Mo_xW_{1-x}S_2$ was avoided by a precise control of the reaction temperature: vertically stacked bilayers are preferred at 850° C, while in-plane lateral heterojunctions appear at 650 °C.

Metal and chalcogen compounds supplied directly in gaseous phase

In order to achieve a better control of chalcogen supply, a possible route would be the use of H_2S or other S/Se precursors. Nevertheless, no works in literature were found using metal powders and alternative S/Se precursors. For example one may argue that the supply of H_2S may, in principle, offer a better control over the S partial pressure, since the growth and nucleation is sensitive to precursors concentrations and gradients.
H_2S should decompose in S_2 at the typical MoS_2 or WS_2 deposition temperatures, even if the cracking efficiency is low (1-10%) [112].
Also precursors such as dimethil disulfide, dimethil selenide, etc were never considered for reaction with metal powders, at the best of author's knowledge.
A few works exist, however, about the CVD or ALD deposition of TMD using combination of "other" metal and chalcogen precursors described in the corresponding paragraphs. These precursors have high vapour pressure and are stored in liquid or solid forms in canister or bubblers. They are delivered to the growth chamber using a carrier gas and a standard CVD deposition system could be used. As discussed previously, the advantages of this approach are the availability of a well-understood and developed deposition system, the precise control of precursor supply and homogeneity achieved in the growth chamber due to a optimized flowdynamic design, despite the more complex experimental setup needed.
Ideally, the most convenient method for the deposition of monolayer TMD should be ALD, with intrinsic control of layer number and surface reactions. Despite these advantages, very few groups explored the possibilities offered by this technique, yet. A comprehensive study about ALD of metal sulfide was presented by Dasgupta et al. [113] but it was not focussed on transition metals. However, it describes in details several reaction mechanisms involving the reactions of sulfide, observing that ligand-exchange mechanism of surface thiols (−SH) in sulfide ALD should play the same role as surface hydroxyls (−OH) in oxide processes and identifying several challenges, such as ion exchange, air reactivity, and H_2S toxicity, to be addressed in order to incorporate sulfide processes into device manufacturing.
The proposed precursors for the ALD or CVD of MoS_2 are $MoCl_5$, $Mo(CO)_6$, H_2S and dimethyl disulfide (DMDS, $(CH_3)_2S_2$), while WSe_2 was grown using $W(CO)_6$, WCl5 and dimethyl selenium (DMSe, $(CH_3)_2Se$).
Physisorbed $Mo(CO)_6$ undergoes to decarbonylation processes, with the formation of chemisorbed subcarbonyls ($Mo(CO)_n$ $n \leq 5$). For this reason $Mo(CO)_6$ was chosen as a good Mo precursor for the first-half reaction of ALD for MoS_2 synthesis [114]. It was used in combination with both H_2S [115] and DMDS [62]. It is vapourized from room temperature up to 130 °C and delivered into the reactor using N_2 as carrier gas. Doses of $Mo(CO)_6$ and dimethyl disulfide were 1.8×10^{-6} and 4.0×10^{-4} mol s^{-1}, respectively, while Mo:H_2S:(Ar or H_2) ratio were maintained at 1:10:100 or 1:10:1000. Self-limiting process for the ALD processes was verified, and the total number of layers deposited was always found linear with the number of cycles. Generally, growth rates al low as 10 cycles/monolayer were observed, permitting in principle an high degree of control.

ALD chemistry for $Mo(CO)_6$ and DMDS was proposed as [62]:

$$-S + Mo(CO)_{6\,(g)} \rightarrow -S - Mo(CO)_n + (6-n)\,CO_{(g)} \quad (5)$$
$$- Mo(CO)_n + CH_3S_2CH_{3\,(g)} \rightarrow - Mo - S + byproducts_{(g)}$$

where – denotes surface adsorbed species.

The deposition was obtained at temperatures as low as 100 - 140 °C but the flakes were amorphous, even if local S–Mo–S order with an atomic arrangement of 2H-MoS_2 was observed by Raman analysis. A subsequent annealing at 900 °C for 5 min in Ar atmosphere permitted to recrystallize the domains and obtain better Raman signals [62]. Thermodynamic models were developed to understand $Mo(CO)_6$ and H_2S gas phase and deposition chemistry, in order to identify a process windows for CVD deposition of MoS_2 [66] (Fig. 10).

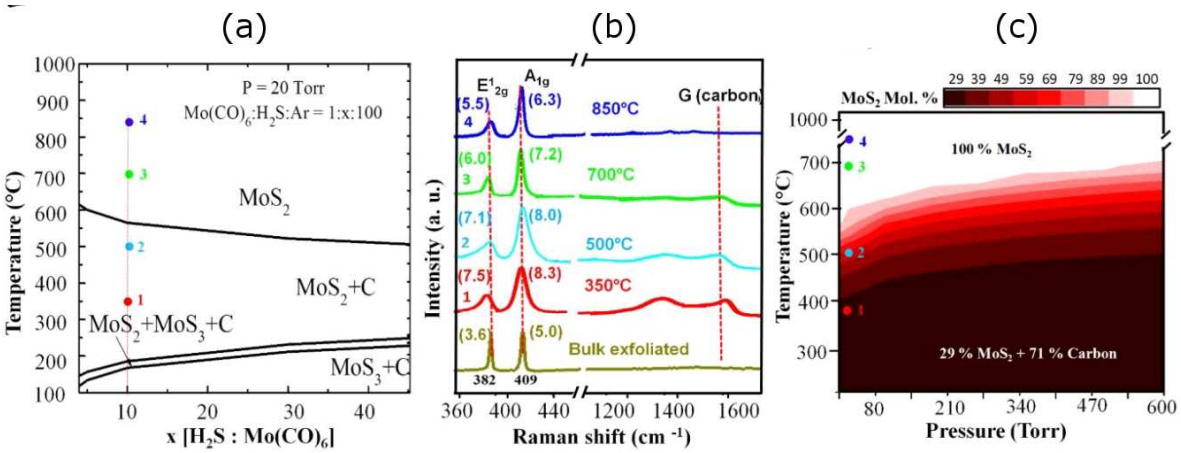

Fig. 10 (a) Calculated stability windows for various condensed phases at P = 20 Torr. (b) Raman spectra (with exfoliated bulk MoS_2 as reference) of multilayer MoS_2 films deposited in argon ambient on sapphire over a wide range of T, with P_{tot} = 20 Torr and $Mo(CO)_6$:H_2S = 1:10 with indices in bracket showing FWHM of corresponding E^1_{2g} and A_{1g} peaks. (c) Contour plot showing the variation in the mole percentage of MoS_2 in the MoS_2-C film at different temperatures and pressures for the composition represented by the dotted line in (a). Reproduced from [66] with permission of The Royal Society of Chemistry.

MoS_2 deposition with characteristic monolayer Raman peaks was obtained only at temperature higher than 350 °C with an optimal setting of 850 °C. The growth parameters were extensively studied and optimal deposition pressure of 500 mbar, gas phase ratio Mo:H_2S of 1:10 and H_2 partial pressure were identified. C contamination was found in the deposited layer, with level depending on total pressure and H_2 content, but was minimized by using temperature of 850 °C. Supersaturation was found to be the most critical parameter to control the number of monolayer. With the precursors concentration used in the paper, a MoS_2 monolayer is obtained in about 1 minute.

$MoCl_5$ was used in combination with H_2S for ALD of MoS_2. It was kept at temperature between 105 and 120 °C to get a sufficient vapour pressure, with N_2 as carrier gas [84], [115]. Deposition temperature was set at 350 °C, 400 °C or 800 °C, with evidence of monolayer formation even in the lowest range. Smooth, uniform, continuous MoS_2 films with remarkable Raman peaks, no visible grain boundaries and strong photoluminescence signal were obtained. However, Tan et al. report that a post-annealing process at 500-800 °C in S vapour permitted to reconstruct the as-grown layers and to improve the crystallinity, as observed by the enhancement of Raman peaks. With the use of $MoCl_5$ and H_2S the number of deposited layers was reported as linear with the number of cycles, with at least 10 cylces needed to obtain a single monolayer.

A similar process was proposed for WS_2 using WCl_5 and H_2S [98]. Large area nanosheets were found after 25 min growth at 700 °C in Ar atmosphere. The domains initially nucleated with small size (100 nm), and later merged to form a continuous film with a layer-by-layer process.
Growth of WSe_2 using $W(CO)_6$ and DMSe was described by Eichfeld et al. [72]. The deposition was controlled by optimizing growth parameters such as temperature, pressure, Se:W ratio, and substrate type. Optimal temperature (900 °C), pressure (700 torr) and Se:W ratio (up to 20.000) settings permitted to obtain size domains up to 8 μm. Amongst the different substrates used for the experiments, epitaxial and CVD graphene gave the highest nucleation density of monolayer WSe_2 domains. The lowest nucleation density was obtained on boron nitride, with preference for vertical (3D) growth of WSe_2 versus lateral (2D) growth. Sapphire provided the largest triangular WSe_2 domains, suggesting that sticking coefficient of adatoms on its surface is higher, as well as their surface mobility. Precursor purity have a significant impact on the film quality, and carbon contamination was reduced by using high purity DMSe. Also, the presence of H_2 promoted WSe_2 growth and permitted to obtain lower C contamination.
Thin WS_2 films were deposited on glass by CVD [68] but the thickness was about 400 nm, so no direct informations about 2D TMD can be obtained from this work. However, this demonstrate that WS_2 can be deposited using precursors such as $W(CO)_6$, WCl_6 $WOCl_4$, 1,2- ethanedithiol [$HS(CH_2)_2SH$] and 2-methylpropanethiol ($HSC(CH_3)_3$) at temperature ranging from 300 to 600 °C and atmospheric pressure. Growth rates up to 400 nm/min at the proposed growth conditions were obtained, with evidence of Volmer-Weber 3D nucleation and WS_2 domains up to 200 nm in size. No evidence of C or Cl contamination was found in the films.

Synthesis of TMD from metal or metal oxides deposited on substrate

One of the most convenient methods to obtain monolayer TMD is, in principle, to deposit a thin metal layer over the substrate, control its thickness in the range 1-5 nm, and then sulfurize it to obtain MoS_2 or WS_2. Drawback of this process is the difficulty to get precise metal thickness and homogeneity over large area. The interaction of sulfur with Mo or W films has been studied extensively, both experimentally and theoretically [116], [117], [118], [119]. Sulfur or MoS_2 powders were used as sulfurizing agent, although also H_2S could be used because its decomposition on Mo metal surface is thermodynamically favoured [118]. The temperatures required for the synthesis of TMD with this method are usually in the range of 750 – 900 °C
Zhan et al. [120] sulfurized a Mo metal film with S powders, forming single and double MoS_2 layer. They found that the thickness of TMD layer is directly related to the thickness of the initial Mo deposited layer. Ma et al [121] observed that the nucleation of MoS_2 on metal substrate is controlled by S supersaturation, which must be lower enough in order to avoid the formation of polycrystalline and defective layer. The use of MoS_2 powder instead of elemental S permitted to reduce the S partial pressure in the vapour phase. This process generally occurs in nitrogen atmosphere, at temperature of about 750 °C.
Vertically aligned MoS_2 and $MoSe_2$ layers were obtained with S or Se powders and an evaporated Mo layer on glassy carbon, quartz, and SiO_2/Si substrates [122]. The rapid sulfurization / selenization processes were performed in Ar at 550 °C: diffusion mechanisms of S and Se into the metal promote the formation of MoS_2 / $MoSe_2$ layers aligned perpendicular to the substrate. Chemical conversion in TMD occurs much faster than the diffusion of S and Se gas, which is then the process limiting factor.
Sulfurization of a thin W or Mo layer deposited on MgO was described by Orofeo et al. [123]. W film was converted to WS_2 via chemical reactions at 800 °C using sulfur powders. No aggregation of the metal into smaller island was observed, due to the fact that the surface energy and mobility of the metal atoms are not high enough at this growth temperature. The characteristics of final TMD flakes were determined by the initial thickness of the metal layer.
Since MoO_3 and WO_3, thanks to a lower melting point, can be more easily deposited by means of evaporation or sputtering than the metal counterparts, they were chosen as alternative starting layer for sulfurization or selenization. Process for DMS synthesis is similar to the previous one: S, Se powders or H_2S are used to sulfurize / selenize the coated substrate.

MoS_2 synthesis from MoO_3 is usually a two step process: a first annealing in S-rich inert atmosphere is performed at 500-600 °C, in order to reduce the oxide to MoO_{3-x}. A second stage follows, with MoS_2 formation at higher temperature (850-1000 °C):

$$MoO_{3\,(s)} + S_{(g)} \rightarrow MoO_{3-x\,(s)} + SOx_{(g)} \quad (6)$$
$$MoO_{3-x\,(s)} + S_{(g)} \rightarrow MoS_{2\,(s)}$$

The synthesis was also performed in mixed Ar-H_2 atmosphere [79]. The reactions were proposed as follows:

$$MoO_{3\,(s)} + H_{2\,(g)} \rightarrow MoO_{2\,(s)} + H_2O_{(g)} \quad (7)$$
$$MoO_{2\,(s)} + S_{(g)} \rightarrow MoS_{2\,(s)} + O_{2\,(g)}$$

Lin et al. also pointed out that the direct sulfurization at high temperature, without the suboxide formation at lower temperature, resulted in MoS_2 films with electrical carrier mobility one magnitude lower.
Since the initial layer must be reduced to a suboxide, selenization of the MoO_3 layer requires the addition of H_2 to the gas phase, as discussed for the synthesis of $MoSe_2$ from powder. In this case the process may be similar to the one described in formula (7) with Se in the place of S for the second half of the reaction.
Sulfurization of WO_3 layer by sulfur powders is performed at temperatures between 750 and 900 °C in argon atmosphere [124], [48]. In this case the two step process to produce WO_{3-x} suboxides was not necessary.

Thiosalts – thiomolybdates

Ammonium thiomolybdates $(NH_4)_2MoS_4$ can be reduced to MoS_3 and, subsequently, to MoS_2 after annealing in N_2 atmosphere [125]. A thin layer of $(NH_4)_2MoS_4$ is usually deposited or spin coated over different substrates (SiO_2, quartz, etc) and a two step process is used to synthesis MoS_2. A detailed description of substrate preparation with $(NH_4)_2MoS_4$ is reported in [90]. High temperature annealing of $(NH_4)_2MoS_4$ is likely to result in rapid oxidation, and many reactions are involved in the conversion of $(NH_4)_2MoS_4$ to MoS_2, resulting in irreproducilibty and polycrystalline material with many layers. For this reason, 2 step processes were developed, with an initial annealing at 500 °C and a second heating to 1000 °C in S vapours: the addition of S (through the use of powders) was found to be essential to produce crystalline MoS_2 flakes.

MoS_2 formation is proposed as follows:

$$(NH_4)_2MoS_4 \rightarrow 2\,NH_3 + H_2S + MoS_3 \quad (8)$$
$$MoS_3 \rightarrow MoS_2 + S_2$$

Hydrogen may also play a role in the initial MoS_3 conversion through the reactions [126], [127]:

$$(NH_4)_2MoS_4 + H_2 \rightarrow 2\,NH_3 + 2\,H_2S + MoS_3 \quad (9)$$
$$MoS_3 + H_2 \rightarrow MoS_2 + H_2S$$

H_2 inhibits the etching during film growth and promotes the desulfurization reaction by decreasing the S/Mo atomic ratio and oxidation rate of the MoS_x films.
High quality MoS_2 flakes were obtained by this method, altough the drawback is the difficulty to control the initial $(NH_4)_2MoS_4$ coating of the substrate.

Growth mechanisms

The exact growth processes of TMD are still not fully understood. Several papers propose simple chemical reactions and kinetic mechanisms to explain the synthesis of mono and multi layers, corroborated by theoretical calculations based on density functional theory [41], [79], [107], [128].
As discussed in the previous section, the basic chemical framework is the reduction and further sulfurization / selenization of the metal oxide, with H_2 acting as an additional reducing agent when selenium is involved. H_2 may directly reduce MO_x or it can react with S to produce H_2S: the exact reaction pathway is still under investigation but a combination of the two processes may indeed occur. The reactions involved in the growth of TMD were summarized in equations (3)-(9).
Both homogeous and heterogeneous reactions may be involved in the growth, and two possible mechanisms were identified:

a) MO_{3-x} species are adsorbed on the substrate and further react with S / Se to form MS_2 / MSe_2
b) MO_{3-x} and chalcogen react heterogeneusly in the gas phase, resulting in MX_2 clusters that are adsorbed on the substrate and then grow laterally or form a bulk depending on the growth conditions. In this case surface mobility plays a crucial role in the growth.

These two mechanisms are in competition and it is difficult to control them accurately, eventually separating their contribute. Temperature controls reaction kinetics, adsorption, desorption, mobility of cluster on the surface and thus it is considered the main parameter affecting these growth mechanisms, altough partial pressure of the precursors plays also a role. Considering the phase diagram of the Mo-O-S system [41], a suitable S partial pressure is needed in order to get a proper reducing atmosphere. If S concentration in the gas phase is either too high or too low the conversion of MoO_3 to suboxides may be strongly inhibited or enhanced, leading to suppression of MoS_2 growth or formation of 3D clusters. For this reason the addition of H_2 to the carrier gas may change chemical equilibrium and help the synthesis process.
Given their molecular structure and chemical bonds, TMD are usually observed in triangular form but complex shapes, resulting from assembling of smaller triangles, may be also observed [104], [129].
Atoms on the flake basal plane have very weak chemical reactivity, while the flake edges have higher free energy and are thus preferred nucleation sites. For this reason, under the favoured growth conditions, the flakes tend to expand laterally, forming monolayer structures.
Through direct in-situ observation by TEM on single and multilayer MoS_2 structures during growth, obtained from MoO_3 on $MgAl_2O_4$ substrates sulfurized by H_2S, Hansen et al. [130] confirmed that step sites either in the substrate or in existing flakes can behave as nucleation centers. An existing MoS_2 flakes is stick on the substrate and expands as MoO_x is converted to MoO_xS_y by sulfurization and migrate on the surface to reach energetically favoured sites on flakes edges. Formation of multilayer or bulk MoS_2 is explained by local higher concentration of MoO_xS_y on the substrate, that lead to an increased transfer of Mo to the MoS_2 basal plane. The overall growth mechanism leading to 2D layered structures is attributed to Van Der Waals epitaxy, which relaxes the lattice matching conditions of the epitaxial layer and permit the synthesis of TMD on a wide variety of substrates [91], [131], [130]. The mechanisms described by Hansen et al. for MoS_2 could apply for other TMD such as WS_2, $MoSe_2$, WSe_2 etc, because of similarities between structures and chemical bonds between these materials.
Superficial energy has an important role in nuclation, migration and chemical reactivity of TMD. This is the reason why the use of surfactants such as graphene oxides or other compounds, described previously, has a great effect in the synthesis of TMD. The presence of additional nucleation sites and the lower surface energy promoted by the pretreatment is able to enhance and promote the growth of monolayer flakes [132].
In order to get a full understanding of TMD growth processes, thermodynamic calculations, kinetic models and eventually density functional theory framework should be considered. The complexity of the system poses several hurdles to the growth process. Even if synthesis methods are conceptually simple, the main the biggest issues that delays the develpoment of TMD devices are the careful control of precursor concentration and temperature gradients, eventually over a large area substrate. Growth of high quality

material requires to control thickness, purity and defects. The defects (point defects, vacancies, impurities) are also controlled by the growth conditions (temperature, precursor vapor pressure).

Conclusions

Transition Metal Dichalcogenides are the most promising class of materials to develop novel device concepts and to scale down transistors, in order to continue to fulfill Moore's Law. Contrary to graphene, they have a finite bandgap in the range 1.4 - 1.9 eV and most of them shows semiconducting behaviour. Despite the promises given by their physical characteristics, a lot of open issues still exist to obtain reliable, reproducible and large scale growth of TMD, with particolar emphasis of heterostructures, doping and ternary compounds. In this review the important topic of bottom up synthesis of TMD has been analyzed and discussed. Description and analysis of the different available precursors for TMD synthesis and on different growth methods from the vapour phase were provided, with particular emphasis to Metal-Organic Chemical Vapour deposition and Atomic Layer Deposition. These growth techniques are the most widespread in the semiconductor industry and are nowadays used in the mass production of a vast class of devices. Integration of TMD with other materials by using these methods would open the possibility to integrate them with current manufacture technology.

Acknowledgements

The author is grateful to dr. Giovanni Attolini for reading the manuscript and for useful suggestions and discussions.

References

[1] "International Technology Roadmap for Semiconductors," *International Technology Roadmap for Semiconductors*. [Online]. Available: http://www.itrs.net/.

[2] D. J. Paul, "Si/SiGe heterostructures: from material and physics to devices and circuits," *Semicond. Sci. Technol.*, vol. 19, no. 10, pp. R75–R108, Oct. 2004.

[3] Patrick J. Quinn, *Silicon Innovation Exploiting Moore Scaling and "More than Moore" Technology*. Cham: Springer International Publishing, 2015.

[4] Y. Xia, P. Yang, Y. Sun, Y. Wu, B. Mayers, B. Gates, Y. Yin, F. Kim, and H. Yan, "One-Dimensional Nanostructures: Synthesis, Characterization, and Applications," *Adv. Mater.*, vol. 15, no. 5, pp. 353–389, Mar. 2003.

[5] A. K. Geim, "Graphene: status and prospects.," *Science*, vol. 324, no. 5934, pp. 1530–4, Jun. 2009.

[6] Y.-M. Lin, K. A. Jenkins, A. Valdes-Garcia, J. P. Small, D. B. Farmer, and P. Avouris, "Operation of graphene transistors at gigahertz frequencies.," *Nano Lett.*, vol. 9, no. 1, pp. 422–6, Jan. 2009.

[7] Y. Liu, X. Dong, and P. Chen, "Biological and chemical sensors based on graphene materials.," *Chem. Soc. Rev.*, vol. 41, no. 6, pp. 2283–307, Mar. 2012.

[8] F. Bonaccorso, L. Colombo, G. Yu, M. Stoller, V. Tozzini, A. C. Ferrari, R. S. Ruoff, and V. Pellegrini, "Graphene, related two-dimensional crystals, and hybrid systems for energy conversion and storage," *Science (80-.).*, vol. 347, no. 6217, pp. 1246501–1246501, Jan. 2015.

[9] P. Vogt, P. De Padova, C. Quaresima, J. Avila, E. Frantzeskakis, M. C. Asensio, A. Resta, B. Ealet, and G. Le Lay, "Silicene: Compelling Experimental Evidence for Graphenelike Two-Dimensional Silicon," *Phys. Rev. Lett.*, vol. 108, no. 15, p. 155501, Apr. 2012.

[10] Z. Ni, Q. Liu, K. Tang, J. Zheng, J. Zhou, R. Qin, Z. Gao, D. Yu, and J. Lu, "Tunable bandgap in silicene and germanene.," *Nano Lett.*, vol. 12, no. 1, pp. 113–8, Jan. 2012.

[11] A. Pakdel, C. Zhi, Y. Bando, and D. Golberg, "Low-dimensional boron nitride nanomaterials," *Mater. Today*, vol. 15, no. 6, pp. 256–265, Jun. 2012.

[12] "Intercalated Layered Materials : F. A. Lévy : 9789027709677." [Online]. Available: http://www.bookdepository.com/Intercalated-Layered-Materials/9789027709677. [Accessed: 03-Jul-2015].

[13] T. F. Connolly, Ed., *Groups IV, V, and VI Transition Metals and Compounds*. Boston, MA: Springer US, 1972.

[14] D. L. Greenaway and R. Nitsche, "Preparation and optical properties of group IV–VI2 chalcogenides having the CdI2 structure," *J. Phys. Chem. Solids*, vol. 26, no. 9, pp. 1445–1458, Sep. 1965.

[15] R. Nitsche, D. F. Sargent, and P. Wild, "Crystal growth of quaternary 122464 chalcogenides by iodine vapor transport," *J. Cryst. Growth*, vol. 1, no. 1, pp. 52–53, Jan. 1967.

[16] R. F. Frindt, "Single Crystals of MoS2 Several Molecular Layers Thick," *J. Appl. Phys.*, vol. 37, p. 1928, 1966.

[17] V. Nicolosi, M. Chhowalla, M. G. Kanatzidis, M. S. Strano, and J. N. Coleman, "Liquid Exfoliation of Layered Materials," *Science (80-.).*, vol. 340, no. 6139, pp. 1226419–1226419, Jun. 2013.

[18] Z. Zeng, T. Sun, J. Zhu, X. Huang, Z. Yin, G. Lu, Z. Fan, Q. Yan, H. H. Hng, and H. Zhang, "An effective method for the fabrication of few-layer-thick inorganic nanosheets.," *Angew. Chem. Int. Ed. Engl.*, vol. 51, no. 36, pp. 9052–6, Sep. 2012.

[19] M. Chhowalla, H. S. Shin, G. Eda, L.-J. Li, K. P. Loh, and H. Zhang, "The chemistry of two-dimensional layered transition metal dichalcogenide nanosheets.," *Nat. Chem.*, vol. 5, no. 4, pp. 263–75, Apr. 2013.

[20] A. Splendiani, L. Sun, Y. Zhang, T. Li, J. Kim, C.-Y. Chim, G. Galli, and F. Wang, "Emerging photoluminescence in monolayer MoS2.," *Nano Lett.*, vol. 10, no. 4, pp. 1271–5, Apr. 2010.

[21] O. V. Yazyev and A. Kis, "MoS2 and semiconductors in the flatland," *Mater. Today*, vol. 18, no. 1, Aug. 2014.

[22] D. Xiao, G.-B. Liu, W. Feng, X. Xu, and W. Yao, "Coupled Spin and Valley Physics in Monolayers of MoS_{2} and Other Group-VI Dichalcogenides," *Phys. Rev. Lett.*, vol. 108, no. 19, p. 196802, May 2012.

[23] H. Zeng, J. Dai, W. Yao, D. Xiao, and X. Cui, "Valley polarization in MoS2 monolayers by optical pumping.," *Nat. Nanotechnol.*, vol. 7, no. 8, pp. 490–3, Aug. 2012.

[24] D. Jariwala, V. K. Sangwan, L. J. Lauhon, T. J. Marks, and M. C. Hersam, "Emerging Device Applications for Semiconducting Two-Dimensional Transition Metal Dichalcogenides," *ACS Nano*, vol. 8, no. 2, pp. 1102–1120, 2014.

[25] B. Radisavljevic, A. Radenovic, J. Brivio, V. Giacometti, and A. Kis, "Single-layer MoS2 transistors.," *Nat. Nanotechnol.*, vol. 6, no. 3, pp. 147–50, Mar. 2011.

[26] H. Wang, L. Yu, Y.-H. Lee, Y. Shi, A. Hsu, M. L. Chin, L.-J. Li, M. Dubey, J. Kong, and T. Palacios, "Integrated circuits based on bilayer MoS_2 transistors.," *Nano Lett.*, vol. 12, no. 9, pp. 4674–80, Sep. 2012.

[27] J. K. Huang, J. Pu, C. L. Hsu, M. H. Chiu, Z. Y. Juang, Y. H. Chang, W. H. Chang, Y. Iwasa, T. Takenobu, and L. J. Li, "Large-area synthesis of highly crystalline WSe2 monolayers and device applications," *ACS Nano*, vol. 8, no. 1, pp. 923–930, 2014.

[28] W. Choi, M. Y. Cho, A. Konar, J. H. Lee, G.-B. Cha, S. C. Hong, S. Kim, J. Kim, D. Jena, J. Joo, and S. Kim, "High-detectivity multilayer MoS(2) phototransistors with spectral response from ultraviolet to infrared.," *Adv. Mater.*, vol. 24, no. 43, pp. 5832–6, Nov. 2012.

[29] N. Perea-López, A. L. Elías, A. Berkdemir, A. Castro-Beltran, H. R. Gutiérrez, S. Feng, R. Lv, T. Hayashi, F. López-Urías, S. Ghosh, B. Muchharla, S. Talapatra, H. Terrones, and M. Terrones, "Photosensor Device Based on Few-Layered WS 2 Films," *Adv. Funct. Mater.*, vol. 23, no. 44, pp. 5511–5517, Nov. 2013.

[30] M. Pumera and A. H. Loo, "Layered transition-metal dichalcogenides (MoS2 and WS2) for sensing and biosensing," *TrAC Trends Anal. Chem.*, vol. 61, pp. 49–53, Oct. 2014.

[31] A.-J. Cho, K. C. Park, and J.-Y. Kwon, "A high-performance complementary inverter based on transition metal dichalcogenide field-effect transistors.," *Nanoscale Res. Lett.*, vol. 10, p. 115, Jan. 2015.

[32] F. Withers, O. Del Pozo-Zamudio, a. Mishchenko, a. P. Rooney, a. Gholinia, K. Watanabe, T. Taniguchi, S. J. Haigh, a. K. Geim, a. I. Tartakovskii, and K. S. Novoselov, "Light-emitting diodes by band-structure engineering in van der Waals heterostructures," *Nat. Mater.*, vol. 14, no. February, pp. 301–306, 2015.

[33] Q. He, Z. Zeng, Z. Yin, H. Li, S. Wu, X. Huang, and H. Zhang, "Fabrication of flexible MoS2 thin-film transistor arrays for practical gas-sensing applications.," *Small*, vol. 8, no. 19, pp. 2994–9, Oct. 2012.

[34] H.-P. Komsa and A. V. Krasheninnikov, "Effects of confinement and environment on the electronic structure and exciton binding energy of MoS 2 from first principles," *Phys. Rev. B*, vol. 86, no. 24, p. 241201, Dec. 2012.

[35] Q. Zeng, H. Wang, W. Fu, Y. Gong, W. Zhou, P. M. Ajayan, J. Lou, and Z. Liu, "Band Engineering for Novel Two-Dimensional Atomic Layers," *Small*, pp. 1–17, 2014.

[36] S.-H. Su, Y.-T. Hsu, Y.-H. Chang, M.-H. Chiu, C.-L. Hsu, W.-T. Hsu, W.-H. Chang, J.-H. He, and L.-J. Li, "Band gap-tunable molybdenum sulfide selenide monolayer alloy.," *Small*, vol. 10, no. 13, pp. 2589–94, Jul. 2014.

[37] S. Das, M. Kim, J. Lee, and W. Choi, "Synthesis, Properties, and Applications of 2-D Materials: A Comprehensive Review," *Crit. Rev. Solid State Mater. Sci.*, vol. 39, no. March 2015, pp. 231–252, 2014.

[38] Q. H. Wang, K. Kalantar-Zadeh, A. Kis, J. N. Coleman, and M. S. Strano, "Electronics and optoelectronics of two-dimensional transition metal dichalcogenides.," *Nat. Nanotechnol.*, vol. 7, no. 11, pp. 699–712, 2012.

[39] S. Z. Butler, S. M. Hollen, L. Cao, Y. Cui, J. a. Gupta, H. R. Gutiérrez, T. F. Heinz, S. S. Hong, J. Huang, A. F. Ismach, E. Johnston-Halperin, M. Kuno, V. V. Plashnitsa, R. D. Robinson, R. S. Ruoff, S. Salahuddin, J. Shan, L. Shi, M. G. Spencer, M. Terrones, W. Windl, and J. E. Goldberger, "Progress, challenges, and opportunities in two-dimensional materials beyond graphene," *ACS Nano*, vol. 7, no. 4, pp. 2898–2926, 2013.

[40] Y. Shi, H. Li, and L.-J. Li, "Recent advances in controlled synthesis of two-dimensional transition metal dichalcogenides via vapour deposition techniques," *Chem. Soc. Rev.*, Oct. 2014.

[41] Q. Ji, Y. Zhang, Y. Zhang, and Z. Liu, "Chemical vapour deposition of group-VIB metal dichalcogenide monolayers: engineered substrates from amorphous to single crystalline.," *Chem. Soc. Rev.*, 2014.

[42] R. Lv, J. a Robinson, R. E. Schaak, D. Sun, Y. Sun, T. E. Mallouk, and M. Terrones, "Transition Metal Dichalcogenides and Beyond: Synthesis, Properties, and Applications of Single- and Few-Layer Nanosheets," *Acc. Chem. Res.*, 2014.

[43] X. Li and H. Zhu, "Two-dimensional MoS2: Properties, preparation, and applications," *J. Mater.*, vol. 1, no. 1, pp. 33–44, Mar. 2015.

[44] G. Fiori, F. Bonaccorso, G. Iannaccone, T. Palacios, D. Neumaier, A. Seabaugh, S. K. Banerjee, and L. Colombo, "Electronics based on two-dimensional materials," *Nat. Nanotechnol.*, vol. 9, no. October, pp. 768–779, 2014.

[45] P. Tonndorf, R. Schmidt, P. Böttger, X. Zhang, J. Börner, A. Liebig, M. Albrecht, C. Kloc, O. Gordan, D. R. T. Zahn, S. Michaelis de Vasconcellos, and R. Bratschitsch, "Photoluminescence emission and Raman response of monolayer MoS_2, $MoSe_2$, and WSe_2.," *Opt. Express*, vol. 21, no. 4, pp. 4908–16, Feb. 2013.

[46] A. Berkdemir, H. R. Gutiérrez, A. R. Botello-Méndez, N. Perea-López, A. L. Elías, C.-I. Chia, B. Wang, V. H. Crespi, F. López-Urías, J.-C. Charlier, H. Terrones, and M. Terrones, "Identification of individual and few layers of WS2 using Raman Spectroscopy," *Sci. Rep.*, vol. 3, Apr. 2013.

[47] X. Luo, Y. Zhao, J. Zhang, M. Toh, C. Kloc, Q. Xiong, and S. Y. Quek, "Effects of lower symmetry and dimensionality on Raman spectra in two-dimensional WSe 2," *Phys. Rev. B*, vol. 88, no. 19, p. 195313, Nov. 2013.

[48] H. R. Gutiérrez, N. Perea-López, A. L. Elías, A. Berkdemir, B. Wang, R. Lv, F. López-Urías, V. H. Crespi, H. Terrones, and M. Terrones, "Extraordinary room-temperature photoluminescence in triangular WS2 monolayers.," *Nano Lett.*, vol. 13, no. 8, pp. 3447–54, Aug. 2013.

[49] M. M. Benameur, B. Radisavljevic, J. S. Héron, S. Sahoo, H. Berger, and A. Kis, "Visibility of dichalcogenide nanolayers.," *Nanotechnology*, vol. 22, no. 12, p. 125706, Mar. 2011.

[50] J. N. Coleman, M. Lotya, A. O'Neill, S. D. Bergin, P. J. King, U. Khan, K. Young, A. Gaucher, S. De, R. J. Smith, I. V Shvets, S. K. Arora, G. Stanton, H.-Y. Kim, K. Lee, G. T. Kim, G. S. Duesberg, T. Hallam, J. J. Boland, J. J. Wang, J. F. Donegan, J. C. Grunlan, G. Moriarty, A. Shmeliov, R. J. Nicholls, J. M. Perkins, E. M. Grieveson, K. Theuwissen, D. W. McComb, P. D. Nellist, and V. Nicolosi, "Two-dimensional nanosheets produced by liquid exfoliation of layered materials.," *Science*, vol. 331, no. 6017, pp. 568–71, Feb. 2011.

[51] R. J. Smith, P. J. King, M. Lotya, C. Wirtz, U. Khan, S. De, A. O'Neill, G. S. Duesberg, J. C. Grunlan, G. Moriarty, J. Chen, J. Wang, A. I. Minett, V. Nicolosi, and J. N. Coleman, "Large-scale exfoliation of inorganic layered compounds in aqueous surfactant solutions.," *Adv. Mater.*, vol. 23, no. 34, pp. 3944–8, Sep. 2011.

[52] Z. Zeng, Z. Yin, X. Huang, H. Li, Q. He, G. Lu, F. Boey, and H. Zhang, "Single-layer semiconducting nanosheets: high-yield preparation and device fabrication.," *Angew. Chem. Int. Ed. Engl.*, vol. 50, no. 47, pp. 11093–7, Nov. 2011.

[53] H. Fang, S. Chuang, T. C. Chang, K. Takei, T. Takahashi, and A. Javey, "High-performance single layered WSe_2 p-FETs with chemically doped contacts.," *Nano Lett.*, vol. 12, no. 7, pp. 3788–92, Jul. 2012.

[54] K. S. Novoselov, D. Jiang, F. Schedin, T. J. Booth, V. V Khotkevich, S. V Morozov, and A. K. Geim, "Two-dimensional atomic crystals.," *Proc. Natl. Acad. Sci. U. S. A.*, vol. 102, no. 30, pp. 10451–3, Jul. 2005.

[55] M. A. Ibrahem, W.-C. Huang, T. Lan, K. M. Boopathi, Y.-C. Hsiao, C.-H. Chen, W. Budiawan, Y.-Y. Chen, C.-S. Chang, L.-J. Li, C.-H. Tsai, and C. W. Chu, "Controlled mechanical cleavage of bulk niobium diselenide to nanoscaled sheet, rod, and particle structures for Pt-free dye-sensitized solar cells," *J. Mater. Chem. A*, vol. 2, no. 29, p. 11382, Jul. 2014.

[56] I. G. Lezama, A. Arora, A. Ubaldini, C. Barreteau, E. Giannini, M. Potemski, and A. Morpurgo, "Indirect-to-direct band-gap crossover in few-layer MoTe2.," *Nano Lett.*, vol. 15, no. 4, pp. 2336–2342, Mar. 2015.

[57] K. Xu, P. Chen, X. Li, C. Wu, Y. Guo, J. Zhao, X. Wu, and Y. Xie, "Ultrathin nanosheets of vanadium diselenide: a metallic two-dimensional material with ferromagnetic charge-density-wave behavior.," *Angew. Chem. Int. Ed. Engl.*, vol. 52, no. 40, pp. 10477–81, Sep. 2013.

[58] E. Benavente, "Intercalation chemistry of molybdenum disulfide," *Coord. Chem. Rev.*, vol. 224, no. 1–2, pp. 87–109, Jan. 2002.

[59] A. S. Golub', Y. V. Zubavichus, Y. L. Slovokhotov, and Y. N. Novikov, "Single-layer dispersions of transition metal dichalcogenides in the synthesis of intercalation compounds," *Russ. Chem. Rev.*, vol. 72, no. 2, pp. 123–141, Apr. 2003.

[60] X. Li, W. Cai, J. An, S. Kim, J. Nah, D. Yang, R. Piner, A. Velamakanni, I. Jung, E. Tutuc, S. K. Banerjee, L. Colombo, and R. S. Ruoff, "Large-area synthesis of high-quality and uniform graphene films on copper foils.," *Science*, vol. 324, no. 5932, pp. 1312–4, Jun. 2009.

[61] T. Suntola, "Atomic layer epitaxy," *Mater. Sci. Reports*, vol. 4, no. 5, pp. 261–312, Jan. 1989.

[62] Z. Jin, S. Shin, D. H. Kwon, S.-J. Han, and Y.-S. Min, "Novel chemical route for atomic layer deposition of MoS thin film on SiO/Si substrate," *Nanoscale*, vol. 6, no. 23, pp. 14453–8, Nov. 2014.

[63] B. Meyer, “Elemental sulfur,” *Chem. Rev.*, vol. 76, no. 3, pp. 367–387, 1976.

[64] N. P. Dasgupta, J. F. Mack, M. C. Langston, A. Bousetta, and F. B. Prinz, “Design of an atomic layer deposition reactor for hydrogen sulfide compatibility.,” *Rev. Sci. Instrum.*, vol. 81, no. 4, p. 044102, Apr. 2010.

[65] E. D. C. Zachary R. Robinson, Scott W. Schmucker, Kathleen M. McCreary, “Chemical Vapor Deposition of Two-Dimensional Crystals,” in *Handbook of Crystal Growth (Second Edition)*, T. Kuech, Ed. Elsevier B.V., 2015, pp. 785–833.

[66] V. Kranthi Kumar, S. Dhar, T. H. Choudhury, S. a. Shivashankar, and S. Raghavan, “Predictive approach to CVD of crystalline layers of TMDs: The case of MoS2,” *Nanoscale*, 2015.

[67] J. Song, J. Park, W. Lee, T. Choi, H. Jung, C. W. Lee, S. Hwang, J. M. Myoung, J. Jung, S. Kim, C. Lansalot-matras, and H. Kim, “Conformal Synthesis of Tungsten Disul fi de Nanosheets Using Atomic Layer Deposition,” pp. 11333–11340, 2013.

[68] C. J. Carmalt, I. P. Parkin, and E. S. Peters, “Atmospheric pressure chemical vapour deposition of WS2 thin films on glass,” *Polyhedron*, vol. 22, no. 11, pp. 1499–1505, Jun. 2003.

[69] L. S. Brooks, “The Vapor Pressures of Tellurium and Selenium,” *J. Am. Chem. Soc.*, vol. 74, no. 1, pp. 227–229, Jan. 1952.

[70] I. L. Shabalin, *Table 3.8 in Ultra-High Temperature Materials I Carbon (Graphene/Graphite) and Refractory Metals*. 2014.

[71] F. Bozheyev, D. Friedrich, M. Nie, M. Rengachari, and K. Ellmer, “Preparation of highly (001)-oriented photoactive tungsten diselenide (WSe 2) films by an amorphous solid-liquid-crystalline solid (aSLcS) rapid-crystallization process,” *Phys. status solidi*, vol. 211, no. 9, pp. 2013–2019, Sep. 2014.

[72] S. M. Eichfeld, L. Hossain, Y. Lin, A. F. Piasecki, B. Kupp, A. G. Birdwell, R. A. Burke, N. Lu, X. Peng, J. Li, A. Azcatl, S. Mcdonnell, R. M. Wallace, M. J. Kim, T. S. Mayer, J. M. Redwing, and J. A. Robinson, “Highly Scalable , Atomically Thin WSe2 Grown via Metal Organic Chemical Vapor Deposition,” no. 2, pp. 2080–2087, 2015.

[73] U. Karlson, W. T. Frankenberger, and W. F. Spencer, “Physicochemical properties of dimethyl selenide and dimethyl diselenide,” *J. Chem. Eng. Data*, vol. 39, no. 3, pp. 608–610, Jul. 1994.

[74] N. D. Boscher, C. J. Carmalt, and I. P. Parkin, “Atmospheric pressure chemical vapor deposition of WSe 2 thin films on glass—highly hydrophobic sticky surfaces,” *J. Mater. Chem.*, vol. 16, no. 1, pp. 122–127, Dec. 2006.

[75] Y. N. Yoshio Tanaka, “Vapour Pressures of Diethyl Selenide, Tetramethyl Tin and Tetramethyl Lead,” *Proc. Imp. Acad.*, p. 78, Mar. 2008.

[76] N. D. Boscher, C. S. Blackman, C. J. Carmalt, I. P. Parkin, and A. G. Prieto, “Atmospheric pressure chemical vapour deposition of vanadium diselenide thin films,” *Appl. Surf. Sci.*, vol. 253, no. 14, pp. 6041–6046, May 2007.

[77] J. B. B. Heyns, J. J. Cruywagen, and K. A. Scott, “Yellow Molybdenum(VI) Oxide Dihydrate,” in *Inorganic Syntheses, Volume 24*, John Wiley & Sons, Inc, 2007.

[78] D. R. Stull, "Vapor Pressure of Pure Substances. Organic and Inorganic Compounds," *Ind. Eng. Chem.*, vol. 39, no. 4, pp. 517–540, Apr. 1947.

[79] Y.-C. Lin, W. Zhang, J.-K. Huang, K.-K. Liu, Y.-H. Lee, C.-T. Liang, C.-W. Chu, and L.-J. Li, "Wafer-scale MoS2 thin layers prepared by MoO3 sulfurization.," *Nanoscale*, vol. 4, no. 20, pp. 6637–41, Oct. 2012.

[80] M. Diskus, O. Nilsen, and H. Fjellvåg, "Growth of thin films of molybdenum oxide by atomic layer deposition," *J. Mater. Chem.*, vol. 21, no. 3, p. 705, 2011.

[81] J. Lu, H. Hugosson, O. Eriksson, L. Nordström, and U. Jansson, "Chemical vapour deposition of molybdenum carbides: aspects of phase stability," *Thin Solid Films*, vol. 370, no. 1–2, pp. 203–212, Jul. 2000.

[82] Y. Yu, C. Li, Y. Liu, L. Su, Y. Zhang, L. Cao, and I. Facility, "Controlled Scalable Synthesis of Uniform, High-Quality Monolayer and Few- layer."

[83] J. Mann, D. Sun, Q. Ma, J.-R. Chen, E. Preciado, T. Ohta, B. Diaconescu, K. Yamaguchi, T. Tran, M. Wurch, K. Magnone, T. F. Heinz, G. L. Kellogg, R. Kawakami, and L. Bartels, "Facile growth of monolayer MoS2 film areas on SiO2," *Eur. Phys. J. B*, vol. 86, no. 5, p. 226, May 2013.

[84] L. K. Tan, B. Liu, J. H. Teng, S. Guo, H. Y. Low, and K. P. Loh, "Atomic layer deposition of a MoS 2 film," pp. 10584–10588, 2014.

[85] D. Seghete, G. B. Rayner, A. S. Cavanagh, V. R. Anderson, and S. M. George, "Molybdenum Atomic Layer Deposition Using MoF6 and Si2H6 as the Reactants," pp. 1668–1678, 2011.

[86] W. Y. Lee and K. L. More, "Crystal orientation and near-interface structure of chemically vapor deposited MoS2 films," *J. Mater. Res.*, vol. 10, no. 01, pp. 49–53, Mar. 2011.

[87] Y. W. Bae, W. Y. Lee, C. S. Yust, P. J. Blau, and T. M. Besmann, "Synthesis and Friction Behavior of Chemically Vapor Deposited Composite Coatings Containing Discrete TiN and MoS2 Phases," *J. Am. Ceram. Soc.*, vol. 79, no. 4, pp. 819–824, Apr. 1996.

[88] V. Miikkulainen, M. Suvanto, and T. a. Pakkanen, "Bis(tert-butylimido)-bis(dialkylamido) Complexes of Molybdenum as Atomic Layer Deposition (ALD) Precursors for Molybdenum Nitride: the Effect of the Alkyl Group," *Chem. Vap. Depos.*, vol. 14, no. 3–4, pp. 71–77, Apr. 2008.

[89] A. Müller, E. Diemann, R. Jostes, and H. Bögge, "Transition Metal Thiometalates: Properties and Significance in Complex and Bioinorganic Chemistry," *Angew. Chemie Int. Ed. English*, vol. 20, no. 11, pp. 934–955, Nov. 1981.

[90] L.-J. L. Keng-Ku Liu, Wenjing Zhang Yi-Hsien Lee, Yu-Chuan Lin, Mu-Tung Chang, Ching-Yuan Su, Chia-Seng Chang, Hai Li, Yumeng Shi, Hua Zhang, Chao-Sung Lai, "Growth of Large-Area and Highly Crystalline MoS2 Thin Layers on Insulating Substrates," *Nano Lett.*, 2012.

[91] Y.-C. Lin, N. Lu, N. Perea-Lopez, J. Li, Z. Lin, X. Peng, C. H. Lee, C. Sun, L. Calderin, P. N. Browning, M. S. Bresnehan, M. J. Kim, T. S. Mayer, M. Terrones, and J. a Robinson, "Direct synthesis of van der Waals solids.," *ACS Nano*, vol. 8, no. 4, pp. 3715–23, 2014.

[92] R. Morrish, T. Haak, and C. A. Wolden, "Low-Temperature Synthesis of n -Type WS 2 Thin Films via H 2 S Plasma Sulfurization of WO 3," *Chem. Mater.*, vol. 26, no. 13, pp. 3986–3992, Jul. 2014.

[93] T. W. Scharf, S. V. Prasad, M. T. Dugger, P. G. Kotula, R. S. Goeke, and R. K. Grubbs, "Growth, structure, and tribological behavior of atomic layer-deposited tungsten disulphide solid lubricant coatings with applications to MEMS," *Acta Mater.*, vol. 54, pp. 4731–4743, 2006.

[94] R. K. Grubbs, N. J. Steinmetz, and S. . George, "Gas phase reaction products during tungsten atomic layer deposition using WF6 and Si2H6," *J. Vac. Sci. Technol. B*, vol. 22, no. 4, pp. 1811–1821, 2004.

[95] C.-Y. Kim, J. W. Elam, M. J. Pellin, D. K. Goswami, S. T. Christensen, M. C. Hersam, P. C. Stair, and M. J. Bedzyk, "Imaging of atomic layer deposited (ALD) tungsten monolayers on alpha-TiO2(110) by X-ray standing wave Fourier inversion.," *J. Phys. Chem. B*, vol. 110, no. 25, pp. 12616–20, Jun. 2006.

[96] J. Malm, T. Sajavaara, and M. Karppinen, "Atomic Layer Deposition of WO3 Thin Films using W(CO)6 and O3 Precursors," *Chem. Vap. Depos.*, vol. 18, no. 7–9, pp. 245–248, Sep. 2012.

[97] "http://luxel.com/wp-content/uploads/2013/04/Luxel-Vapor-Pressure-Chart.pdf." .

[98] J. Park, W. Lee, T. Choi, S.-H. Hwang, J. M. Myoung, J.-H. Jung, S.-H. Kim, and H. Kim, "Layer-modulated synthesis of uniform tungsten disulfide nanosheet using gas-phase precursors," *Nanoscale*, vol. 7, pp. 1308–1313, Dec. 2015.

[99] A. C. Anacleto, N. Blasco, A. Pinchart, Y. Marot, and C. Lachaud, "Novel cyclopentadienyl based precursors for CVD of W containing films," *Surf. Coatings Technol.*, vol. 201, no. 22–23 SPEC. ISS., pp. 9120–9124, 2007.

[100] N. R. Pradhan, D. Rhodes, S. Feng, Y. Xin, B. Moon, H. Terrones, M. Terrones, and L. Balicas, "Field-Effect Transistors Based on Few-Layered alpha-MoTe2," *ACS Nano*, vol. 8, no. 6, pp. 5911–5920, 2014.

[101] S. Tongay, H. Sahin, C. Ko, A. Luce, W. Fan, K. Liu, J. Zhou, Y.-S. Huang, C.-H. Ho, J. Yan, D. F. Ogletree, S. Aloni, J. Ji, S. Li, J. Li, F. M. Peeters, and J. Wu, "Monolayer behaviour in bulk ReS2 due to electronic and vibrational decoupling.," *Nat. Commun.*, vol. 5, p. 3252, Jan. 2014.

[102] H. Liu, K. K. A. Antwi, S. Chua, and D. Chi, "Vapor-phase growth and characterization of Mo(1-x)W(x)S2 ($0 \le x \le 1$) atomic layers on 2-inch sapphire substrates.," *Nanoscale*, vol. 6, no. 1, pp. 624–9, Jan. 2014.

[103] Y. Rong, Y. Fan, A. Leen Koh, A. W. Robertson, K. He, S. Wang, H. Tan, R. Sinclair, and J. H. Warner, "Controlling sulphur precursor addition for large single crystal domains of WS 2," *Nanoscale*, vol. 6, no. 20, pp. 12096–12103, 2014.

[104] Y. Zhang, Y. Zhang, Q. Ji, J. Ju, H. Yuan, J. Shi, T. Gao, D. Ma, M. Liu, Y. Chen, X. Song, H. Y. Hwang, Y. Cui, and Z. Liu, "Controlled Growth of High-Quality Monolayer WS 2 Layers on Sapphire," *ACS Nano*, vol. 7, no. 10, pp. 8963–8971, 2013.

[105] Y.-H. Lee, X.-Q. Zhang, W. Zhang, M.-T. Chang, C.-T. Lin, K.-D. Chang, Y.-C. Yu, J. T.-W. Wang, C.-S. Chang, L.-J. Li, and T.-W. Lin, "Synthesis of large-area MoS2 atomic layers with chemical vapor deposition.," *Adv. Mater.*, vol. 24, pp. 2320–5, 2012.

[106] J. C. Shaw, H. Zhou, Y. Chen, N. O. Weiss, Y. Liu, Y. Huang, and X. Duan, "Chemical vapor deposition growth of monolayer MoSe2 nanosheets," *Nano Res.*, vol. 7, no. 4, pp. 1–7, 2014.

[107] T. Tsirlina, Y. Feldman, M. Homyonfer, J. Sloan, J. L. Hutchison, and R. Tenne, “Synthesis and characterization of inorganic fullerene-like WSe 2 material,” *Fuller. Sci. Technol.*, vol. 6, no. 1, pp. 157–165, 1998.

[108] X. Ling, Y.-H. Lee, Y. Lin, W. Fang, L. Yu, M. S. Dresselhaus, and J. Kong, “Role of the Seeding Promoter in MoS 2 Growth by Chemical Vapor Deposition,” *Nano Lett.*, vol. 14, no. 2, p. 140129131422004, 2014.

[109] A. M. van der Zande, P. Y. Huang, D. a Chenet, T. C. Berkelbach, Y. You, G.-H. Lee, T. F. Heinz, D. R. Reichman, D. a Muller, and J. C. Hone, “Grains and grain boundaries in highly crystalline monolayer molybdenum disulphide.,” *Nat. Mater.*, vol. 12, no. 6, pp. 554–61, 2013.

[110] Y. Yu, C. Li, Y. Liu, L. Su, Y. Zhang, and L. Cao, “Controlled scalable synthesis of uniform, high-quality monolayer and few-layer MoS2 films.,” *Sci. Rep.*, vol. 3, p. 1866, 2013.

[111] Y. Gong, J. Lin, X. Wang, G. Shi, S. Lei, Z. Lin, X. Zou, G. Ye, R. Vajtai, B. I. Yakobson, H. Terrones, M. Terrones, B. K. Tay, J. Lou, S. T. Pantelides, Z. Liu, W. Zhou, and P. M. Ajayan, “Vertical and in-plane heterostructures from WS2/MoS2 monolayers,” *Nat. Mater.*, vol. 13, no. September, 2014.

[112] K. Karan, A. K. Mehrotra, and L. a. Behie, “On reaction kinetics for the thermal decomposition of hydrogen sulfide,” *AIChE J.*, vol. 45, no. 2, pp. 383–389, 1999.

[113] N. P. Dasgupta, X. Meng, J. W. Elam, and A. B. F. Martinson, “Atomic Layer Deposition of Metal Sulfide Materials,” *Acc. Chem. Res.*, vol. 48, no. 2, pp. 341–348, Feb. 2015.

[114] P. Krüger, M. Petukhov, B. Domenichini, A. Berkó, and S. Bourgeois, “Monolayer Formation of Molybdenum Carbonyl on Cu(111) Revealed by Scanning Tunneling Microscopy and Density Functional Theory,” *J. Phys. Chem. C*, vol. 116, no. 19, pp. 10617–10622, May 2012.

[115] R. Browning, P. Padigi, R. Solanki, D. J. Tweet, P. Schuele, and D. Evans, “Atomic layer deposition of MoS 2 thin films,” *Mater. Res. Express*, vol. 2, no. 3, p. 035006, Feb. 2015.

[116] J. M. Wilson, “LEED and AES study of the interaction of H2S and Mo (100),” *Surf. Sci.*, vol. 53, no. 1, pp. 330–340, Dec. 1975.

[117] M. Salmeron, G. A. Somorjai, and R. R. Chianelli, “A leed-aes study of the structure of sulfur monolayers on the Mo(100) crystal face,” *Surf. Sci.*, vol. 127, no. 3, pp. 526–540, May 1983.

[118] H. Luo, J. Cai, X. Tao, and M. Tan, “Adsorption and dissociation of H2S on Mo(100) surface by first-principles study,” *Appl. Surf. Sci.*, vol. 292, pp. 328–335, Feb. 2014.

[119] D. R. Mullins, P. F. Lyman, and S. H. Overbury, “Interaction of S with W(001),” *Surf. Sci.*, vol. 277, no. 1–2, pp. 64–76, Oct. 1992.

[120] Y. Zhan, Z. Liu, S. Najmaei, P. M. Ajayan, and J. Lou, “Large-area vapor-phase growth and characterization of MoS(2) atomic layers on a SiO(2) substrate.,” *Small*, vol. 8, no. 7, pp. 966–71, Apr. 2012.

[121] L. Ma, D. N. Nath, E. W. Lee, C. H. Lee, A. Arehart, S. Rajan, and Y. Wu, “Epitaxial Growth of Large Area Single-Crystalline Few-Layer MoS2 with Room Temperature Mobility of 192 cm2V-1s-1,” 2014.

[122] D. Kong, H. Wang, J. J. Cha, M. Pasta, K. J. Koski, J. Yao, and Y. Cui, "Synthesis of MoS 2 and MoSe 2 Films with Vertically Aligned Layers," *Nano Lett.*, vol. 13, no. 3, pp. 1341–1347, Mar. 2013.

[123] C. M. Orofeo, S. Suzuki, Y. Sekine, and H. Hibino, "Scalable synthesis of layer-controlled WS2 and MoS2 sheets by sulfurization of thin metal films," *Appl. Phys. Lett.*, vol. 105, no. 8, p. 083112, Aug. 2014.

[124] A. L. Elías, N. Perea-López, A. Castro-Beltrán, A. Berkdemir, R. Lv, S. Feng, A. D. Long, T. Hayashi, Y. A. Kim, M. Endo, H. R. Gutiérrez, N. R. Pradhan, L. Balicas, T. E. Mallouk, F. López-Urías, H. Terrones, and M. Terrones, "Controlled synthesis and transfer of large-area WS2 sheets: from single layer to few layers.," *ACS Nano*, vol. 7, no. 6, pp. 5235–42, Jun. 2013.

[125] J. L. Brito, M. Ilija, and P. Hernández, "Thermal and reductive decomposition of ammonium thiomolybdates," *Thermochim. Acta*, vol. 256, no. 2, pp. 325–338, Jun. 1995.

[126] J. Whelan, I. Banu, G. E. Luckachan, N. D. Banu, S. Stephen, A. Tharalekshmy, S. Al Hashimi, R. V Vladea, M. S. Katsiotis, and S. M. Alhassan, "Influence of decomposition time and H2 pressure on properties of unsupported ammonium tetrathiomolybdate-derived MoS2 catalysts," *J. Anal. Sci. Technol.*, vol. 6, no. 1, p. 8, Feb. 2015.

[127] X. Lee, X. Li, X. Zang, M. Zhu, Y. He, K. Wang, D. Xie, and H. Zhu, "Role of hydrogen in chemical vapor deposition growth of MoS2 atomic layers," *Nanoscale*, Apr. 2015.

[128] Y. Cheng, K. Yao, Y. Yang, L. Li, Y. Yao, Q. Wang, X. Zhang, Y. Han, and U. Schwingenschlögl, "Van der Waals epitaxial growth of MoS2 on SiO2/Si by chemical vapor deposition," *RSC Adv.*, vol. 3, no. 38, p. 17287, Sep. 2013.

[129] C. Cong, J. Shang, X. Wu, B. Cao, N. Peimyoo, C. Qiu, L. Sun, and T. Yu, "Synthesis and Optical Properties of Large-Area Single-Crystalline 2D Semiconductor WS 2 Monolayer from Chemical Vapor Deposition," *Adv. Opt. Mater.*, vol. 2, no. 2, pp. 131–136, Feb. 2014.

[130] L. P. Hansen, E. Johnson, M. Brorson, and S. Helveg, "Growth Mechanism for Single- and Multi-Layer MoS 2 Nanocrystals," *J. Phys. Chem. C*, vol. 118, no. 39, pp. 22768–22773, Oct. 2014.

[131] F. S. Ohuchi, B. a. Parkinson, K. Ueno, and a. Koma, "Van der Waals epitaxial growth and characterization of MoSe2 thin films on SnS2," *J. Appl. Phys.*, vol. 68, no. 1990, pp. 2168–2175, 1990.

[132] Y.-H. Lee, X.-Q. Zhang, W. Zhang, M.-T. Chang, C.-T. Lin, K.-D. Chang, Y.-C. Yu, J. T.-W. Wang, C.-S. Chang, L.-J. Li, and T.-W. Lin, "Synthesis of large-area MoS2 atomic layers with chemical vapor deposition.," *Adv. Mater.*, vol. 24, no. 17, pp. 2320–5, May 2012.